Geosci. Model Dev., 17, 7365–7399, 2024
https://doi.org/10.5194/gmd-17-7365-2024
© Author(s) 2024. This work is distributed under
the Creative Commons Attribution 4.0 License.

Geoscientific Model Development
Open Access
EGU

Bridging the gap: a new module for human water use in the Community Earth System Model version 2.2.1

Sabin I. Taranu[1], David M. Lawrence[2], Yoshihide Wada[3,4], Ting Tang[3,4], Erik Kluzek[2], Sam Rabin[2], Yi Yao[1], Steven J. De Hertog[1,5], Inne Vanderkelen[6,7,8], and Wim Thiery[1]

[1]Department of Water and Climate, Vrije Universiteit Brussel, Brussels, Belgium
[2]National Center for Atmospheric Research, Climate and Global Dynamics Laboratory, Boulder, CO, USA
[3]Biological and Environmental Science and Engineering Division, King Abdullah University of Science and Technology, Thuwal, Saudi Arabia
[4]Water Security Research Group, Biodiversity and Natural Resources Program, International Institute for Applied Systems Analysis, Laxenburg, Austria
[5]Department of Environment, Q-ForestLab, Universiteit Gent, Ghent, Belgium
[6]Wyss Academy for Nature at the University of Bern, Bern, Switzerland
[7]Climate and Environmental Physics Division, University of Bern, Bern, Switzerland
[8]Oeschger Centre for Climate Change Research, University of Bern, Bern, Switzerland

Correspondence: Sabin I. Taranu (sabin.taranu@vub.be)

Received: 7 February 2024 – Discussion started: 8 April 2024
Revised: 24 August 2024 – Accepted: 28 August 2024 – Published: 17 October 2024

Abstract. Water scarcity is exacerbated by rising water use and climate change, yet state-of-the-art Earth system models typically do not represent human water demand. Here we present an enhancement to the Community Earth System Model (CESM) and its land (CLM5) and river (MOSART) components by introducing sectoral water abstractions. The new module enables a better understanding of water demand and supply dynamics across various sectors, including domestic, livestock, thermoelectric, manufacturing, mining, and irrigation. The module conserves water by integrating abstractions from the land component with river component flows and dynamically calculates daily water scarcity based on local demand and supply. Through land-only simulations spanning 1971–2010, we verify our model against known water scarcity hotspots, historical global water withdrawal trends, and regional variations in water use. Our findings show that non-irrigative sectoral consumption has an insignificant effect on regional climate, while emphasizing the importance of including all sectors for water scarcity assessment capabilities. Despite its advancements, the model's limitations, such as its exclusive focus on river water abstractions, highlight areas for potential future refinement. This research paves the way for a more holistic representation of human–water interactions in ESMs, aiming to inform sustainable water management decisions in an evolving global landscape.

1 Introduction

Human-induced land use modifications, together with water resources management, have substantially impacted the Earth's surface and modified the terrestrial water cycle (Foley et al., 2005; Oki and Kanae, 2006; Wada et al., 2010; Rodell et al., 2018). Water serves multi-functional purposes for humans, including agriculture, industrial processes, domestic use, and ecological services. Over the past century, there has been a significant shift in total human water use, driven primarily by factors such as population growth, industrialization, and urbanization (Shiklomanov, 2000; Vörösmarty et al., 2000; UNESCO, 2021). Towards the future, these drivers are projected to further evolve, influenced by technological advancements, socio-economic transitions, and changing water use patterns, thereby likely leading to heightened water demand (Wada et al., 2016). Already, regions globally grapple with issues of drought and water insecurity, challenges

that underscore the criticality of sustainable water management (Hoekstra et al., 2012; Wada et al., 2013; Trenberth et al., 2014; Famiglietti, 2014; Mekonnen and Hoekstra, 2016; Kummu et al., 2016). Adding complexity to this scenario, anticipated climatic changes, characterized by variable precipitation patterns and altered hydrodynamics, will further strain water supply systems (Milly et al., 2008; Trenberth, 2011; Döll and Schmied, 2012; Arnell and Lloyd-Hughes, 2014).

Deforestation and urbanization not only perturb carbon dynamics but also profoundly alter the hydrological cycle, compromising water availability and quality (Coe et al., 2009; Pan et al., 2011; Seto et al., 2012; Baccini et al., 2017). The expansion of agriculture, driven by human food demands, modifies natural catchments and exacerbates water withdrawals, placing immense stress on both surface and groundwater resources (Wada et al., 2012; Famiglietti, 2014; de Graaf et al., 2019). Such over-extraction has led to phenomena such as land subsidence and saltwater intrusion, which directly threaten the sustainability of freshwater sources (Bierkens and Wada, 2019). The construction of dams and reservoirs, while providing water storage and energy benefits, disrupts riverine ecology, impacts sediment and nutrient transport, modifies natural flow regimes, and can impact local climates (Grill et al., 2015; Best, 2019; Vanderkelen et al., 2021). Pollution, another by-product of human activity, notably from untreated wastewater, poses dire health risks and compromises the integrity of freshwater ecosystems (Vörösmarty et al., 2010). Concurrently, wetland drainage and land reclamation, often undertaken to meet human settlement or agricultural demands, diminish the natural buffering and filtration capacities inherent to these systems (Davidson, 2014). Collectively, these human-driven changes to the land and water nexus not only perturb biogeochemical cycles but also have significant implications for water security, human health, and the socio-economic stability of communities (Bakker, 2012; Link et al., 2016).

The study of the water cycle and broader Earth system changes relies critically on advanced modelling frameworks. Among them, the most integrated are the land surface models (LSMs), which represent the land surface within Earth system models (ESMs) (Blyth et al., 2021). LSMs primarily simulate the interaction between the terrestrial biosphere, atmosphere, and hydrosphere, capturing processes like evapotranspiration, soil moisture dynamics, and snow accumulation and melt. Complementing this, ESMs encapsulate a more comprehensive set of processes and interactions, including atmospheric, oceanic, and cryospheric components, which allow for a holistic examination of the Earth's climatic and environmental dynamics. These models operate over various temporal and spatial scales. At the finer end, some models have spatial resolutions as detailed as a few kilometres, making short-term weather predictions and analysing specific hydrological processes possible (Prein et al., 2015). Conversely, coarser resolutions spanning up to hundreds of kilometres are suitable for long-term climate projections over centuries or millennia (Eyring et al., 2016). Leveraging these scales, researchers can explore a spectrum of phenomena, from short-term flood events to long-term climate change impacts and from localized water table shifts to global sea level rise (Drijfhout et al., 2015; Jevrejeva et al., 2016; Liu et al., 2018; Mankin et al., 2019; Wu et al., 2020). The adaptability and robustness of these frameworks provide invaluable tools for scientists aiming to understand and predict changes in the Earth's water cycle and broader environmental systems.

The field of Earth system modelling has seen important progress between different iterations of the Coupled Model Intercomparison Project phases, demonstrating higher skill in matching observations across relevant climate change indicators (Arias et al., 2021, see Fig. TS.2). This can be attributed to running the models at higher resolutions, increasing model complexity, and improving the representation of physical, chemical, and biological processes (Arias et al., 2021). Despite the progress made, there are still processes not well captured in ESMs. For example, describing human–water interactions was previously recognized as one of the important challenges in Earth system modelling (Nazemi and Wheater, 2015). Recent years, however, have witnessed targeted efforts to bridge this deficiency. This includes the implementation of the land use and land cover change (LULCC) (Lawrence et al., 2016), urban surfaces and associated hydrological disturbances (Lipson et al., 2023), irrigation water use (Blyth et al., 2021; McDermid et al., 2023), large dams and flow regulation (Yassin et al., 2019; Vanderkelen et al., 2021, 2022), and groundwater use (Pokhrel et al., 2016; Nie et al., 2018; Felfelani et al., 2021). A more complete representation of human–water interactions, including abstractions for all sectors from both surface and groundwater sources, as well as reservoir operations, to our knowledge, is currently operationally available for only one ESM system (i.e. MIROC6; Yokohata et al., 2020).

To further contribute to the effort of improving human–water interactions in LSMs/ESMs, we present a new sectoral water use module for the Community Earth System Model version 2 (CESM2) here. Our data-driven module advances the representation of human water use by incorporating a comprehensive account of water abstractions for domestic, livestock, thermoelectric, manufacturing, and mining sectors, thereby complementing the existing irrigation module (Lawrence et al., 2019). Through this development, the CESM2 and its land component more closely approach the capabilities of state-of-the-art global hydrological models (GHMs), which not only represent essential hydrological processes but also commonly integrate human-related water management practices, including reservoir operations, water abstractions, pollution, and the exploration of alternative water sources like desalination and wastewater reuse (Hanasaki et al., 2016; Sutanudjaja et al., 2018; Hanasaki et al., 2018; Burek et al., 2020; Droppers et al., 2020; Müller Schmied et al., 2021; Van Vliet et al., 2021; Jones et al., 2023). Additionally, it enables fully coupled applications, allowing for

the exploration of feedbacks between human water use and land–atmosphere interactions (Keune et al., 2018), which is not achievable with GHMs.

The next section first describes the CESM2 modelling framework with its existing capabilities in representing human–water interactions (Sect. 2.1). Subsequently, a detailed description of the functioning of the new sectoral water use module is given (Sect. 2.2). Next, the information about the prescribed non-irrigative input data is provided (Sect. 2.3). A hypothetical case study is then proposed to better understand the sectoral competition algorithm under limited water availability situations (Sect. 2.4). Since the newly added sectors are data-driven and based on previously evaluated inputs (Huang et al., 2018), the validation section is focused on the robustness of the implementation itself (Sect. 3.1). To assess the capability of the newly developed module, the global and regional trends in sectoral water withdrawal are analysed for the historical period 1973–2010, with a distinction being made between expected and actual fluxes (Sect. 3.2–3.3). The ability of irrigation and other sectors' consumption to impact local climates through changes in surface water–energy exchanges is then investigated (Sect. 3.4). Next, model results are used for a global qualitative water scarcity assessment, showing the model's ability to predict known hotspots of water scarcity (Sect. 3.5). Last, before concluding (Sect. 5), a discussion of existing limitations and possible future refinements is provided (Sect. 4).

2 Methods

2.1 Existing human–water representation in CESM2

The CESM2 is an open-source, community-developed Earth system model that encompasses ocean, atmosphere, land, sea ice, land ice, river, and wave models. These individual models, which may operate at a different spatial resolution and time step, interact and exchange states and fluxes via a coupler (Danabasoglu et al., 2020). Since human water abstractions occur over land, we have focused our model development on the land and river components of the CESM2 model, which are the Community Land Model version 5 (CLM5; Lawrence et al., 2019) and the Model for Scale Adaptive River Transport (MOSART; Li et al., 2013).

CLM5 already models irrigation, with irrigation water abstractions being computed on a daily basis, based on soil moisture deficits and irrigated crop water requirements (Sacks et al., 2009; Lawrence et al., 2019). The default source for water supply for irrigation is the river network, with a user-defined possibility for supply from groundwater. At the moment, however, the simulated groundwater abstractions for irrigation are not constrained by observations, and this new CLM5 module has not been thoroughly tested. Therefore, in this study, we exclusively use the default configuration, where water is abstracted from the river network.

River water availability within CLM5 is provided by the MOSART routing model. It utilizes a kinematic wave approach, providing information on varying channel velocities, water depth in channels, and channel surface water variations (Li et al., 2013). In its functionality, surface runoff from CLM5 first traverses hillslopes before merging with subsurface runoff and moving to a tributary network and finally ending up in the main channel (Fig. 1 in Li et al., 2013). Each MOSART grid cell has a single main channel that connects the local spatial unit with upstream/downstream units through the river network. It is this main channel's water storage, aggregated at CLM5 grid cell level, that is used to estimate current river water availability. It should be noted that the CLM5 and MOSART models can run using different grids, which is the case in this study, with MOSART running on a $0.5 \times 0.5^{\circ}$ grid and CLM5 on a $0.9 \times 1.25^{\circ}$ grid. This means that for a given CLM5 grid cell, several MOSART main channels will be sourced for water supply. The handling of these spatial discrepancies is done through remapping procedures in the coupler.

Once the irrigation water demand is met by abstraction from the river network, it is applied over the surface soil across irrigated crop columns (Fig. A1). This arrangement allows the water to contribute to crop growth and become a part of the surface water–energy balance through processes like evapotranspiration, runoff, and infiltration (Fig. A2). In case there is not enough water to fully satisfy irrigation requirements, the model has two options: first, to limit irrigation abstraction to 90 % of the current river storage, which helps maintain at least 10 % for environmental flow requirements, and second, to abstract as much as needed, with the shortfall being compensated by ocean water. While less realistic, the second setup was successfully used in studies where having the total irrigation requirements satisfied is important (Thiery et al., 2017; Yao et al., 2022).

Recently, additional developments have been completed to advance human water representation in CESM2, notably the dynamically changing open-water surfaces to represent historical reservoir construction (Vanderkelen et al., 2021); the implementation of the Hanasaki et al. (2006) reservoir operation scheme in the vector-based global routing model mizuRoute (Mizukami et al., 2016; Vanderkelen et al., 2022); and the implementation of different irrigation techniques including drip, sprinkler, paddy, and flood (Yao et al., 2022). At the time of publishing this paper, the latter two developments are not yet available for usage in the release version of the CESM2 but are in the process of being integrated.

2.2 New sectoral water use module

The primary focus of our module development is to accurately depict the withdrawal and consumption of water across a variety of sectors. We define withdrawal as the gross amount of water removed from a water source for use in a particular sector. Sectoral water consumption, on the other

hand, is the portion of water withdrawn that is actually consumed and not returned to the water source. It includes water that is lost through evapotranspiration, incorporated into products or crops, or otherwise not returned to the immediate water environment. This is achieved using a data-driven approach. The new module is designed to accept monthly expected water withdrawal and consumption data from non-prognostic sectors (all sectors excluding irrigation; Fig. 1). Expected daily water abstractions are then calculated within the land component of the model, CLM5, at grid cell level (Fig. A1), by assuming a uniform distribution for all days within each month. To satisfy the water demand of each sector, water is provided from the river network and facilitated by a two-way coupling with the MOSART routing model. An existing coupling module between the land and routing components existed already for irrigation purposes. Its functionality was therefore adapted and extended to support the newly added sectors for both withdrawal and return flow fluxes.

During the coupling process, each CLM5 grid cell sends – through the coupler – to MOSART the information about how much water should be withdrawn and how much should be recycled for each sector. The difference between the withdrawal and recycled part is the sectoral consumption, which is the net water amount which is transported from the river system to the land component. The CLM5 and MOSART spatial organization is different in this study, with CLM5 running on a $0.9 \times 1.25°$ grid, while MOSART runs on a $0.5 \times 0.5°$ grid. This needs to be taken into account when passing sectoral fluxes or water storage information from one model to the other during the coupling process.

In CLM5, the spatial land surface heterogeneity is represented through a nested subgrid hierarchy (Fig. A1) (Lawrence et al., 2019). Each grid cell contains multiple land units, columns, plant functional types (PFTs), and crop functional types (CFTs; if the crop option is on). Land units, capturing the broadest patterns, include glacier, lake, urban, vegetated, and crop. Urban units are further divided into density classes. Columns represent the variability within a land unit, such as different soil and snow states. Vegetated units may have multiple columns for soil profiles, while managed vegetation units have irrigated and non-irrigated columns. Columns have up to 25 layers for ground and 10 for snow, which allows solving for water storage and snow dynamics. The PFTs and CFTs corresponding to the third subgrid level, referred to as patches, represent various trees, shrubs, grass, and crop covers that populate the given region. The patch level is intended to capture the biogeophysical and biogeochemical differences between broad categories of plants in terms of their functional characteristics (Lawrence et al., 2019). While the subgrid heterogeneity is captured by the model in the sense of realistic fractions of different land units, PFTs and CFTs, their exact relative location is not represented. The calculations are done individually over each column, and the outputs are then aggregated at grid cell level before exchanging information with the coupler.

MOSART, which operates on its own grid, divides each spatial unit, such as a latitudinal/longitudinal grid cell or a watershed, into three hydrological categories (Fig. 1 in Li et al., 2013): hillslopes that convert both surface and subsurface runoff into tributaries, tributaries that discharge into a single main channel, and the main channel that connects the local spatial unit with upstream/downstream units through the river network (Li et al., 2013).

The information about how much water is potentially available for sectoral use is provided by the coupler to the CLM5 model at the grid cell level by calculating the corresponding total river network storage in the MOSART model. This includes only the liquid water from the rivers, excluding iced river water or the water stored directly in the soils, which are not used to meet sectoral demands. Conversely, to send the information concerning each sector withdrawal and return flow to the MOSART model, a new module was implemented in the coupler codebase that divides the sectoral fluxes across all main channels within the corresponding CLM5 grid cell in accordance with their relative weight in current water storage capacity. In this way, the main channels with larger current water storage will experience higher sectoral use than smaller-capacity channels. For example, if MOSART has two active main channels within a CLM5 grid cell with a total water storage VOLR (variable name in the model), with the larger channel containing 80 % of the VOLR and the smaller channel containing the remaining 20 %, then the sectoral fluxes from the CLM5 grid cell will be distributed across the two available channels in the same proportion (i.e. 80 % and 20 %). The same approach was originally implemented for the irrigation without the return flow part. The new module is therefore a generalization for the remaining sectors.

To simulate idealized scenarios to diagnose instances of water scarcity, the new module implements a basic sectoral priority algorithm for situations when water availability is inadequate to meet the full sectoral demand. Under this system, when water is scarce, it is allocated to sectors in the following priority order: domestic, livestock, thermoelectric, manufacturing, mining, and irrigation. Similar sectoral priority orders have been implemented in some global hydrological models (GHMs; e.g. H08, Hanasaki et al., 2018, and VIC-5, Droppers et al., 2020). This order reflects a general premise that priority should be given to high-value-added products in resource allocation. Municipal, industrial, and agricultural water use intensities per value added are estimated at 0.012, 0.063, and 2.2×10^6 m^3 per USD 1 million, respectively (Hanasaki et al., 2018). This highlights the notion that sectors such as municipal and industrial services provide higher economic returns per unit of water used compared to agriculture (Hanasaki et al., 2018).

It is at this stage that a distinction is made between expected and actual fluxes. Expected withdrawal or consump-

tion is based on input data estimates, while actual withdrawal or consumption represents the fluxes which are computed within the new module after the water availability and sectoral competition are accounted for. Here we should mention that the irrigation and the new sectoral water use modules are kept separated within CLM5, and the abstraction procedures are activated at different stages within the model driving loop. To achieve the connection of the two modules within the sectoral competition algorithm, we activate the abstractions for sectoral use before irrigation is treated and then update the amount of available water perceived by the irrigation module by subtracting the withdrawal which was already done for the other sectors.

After water is allocated to each sector, the new module accounts for the return flow and consumptive use of the water (Fig. 1). A portion of the utilized water is recycled, meaning that it is returned directly to the river network via the MOSART routing model, following the coupling mechanism described previously. The return flow is computed for each sector by subtracting the actual consumption from the actual withdrawal. How much is returned in comparison to the withdrawal depends on the sector and country (Huang et al., 2018). For example, thermoelectric water use has the highest recycling rates, as there are few associated evaporative losses during the power plant's cooling process, while livestock has the lowest (Fig. C2). From a water availability perspective, consumed water is considered "lost", and in this module, it is applied to the surface of soil columns covered with natural vegetation in the CLM5. It is important to mention here that while the sectoral demand for non-irrigative sectors is generated at the grid cell level, the consumption (the net transport of water from the river to the land model) is distributed at a subgrid level on the natural vegetation land unit (Fig. A1). This is done to not interfere with the cropland and urban land units, which have their own soil columns. Thus, sectoral consumption contributes to the surface water–energy balance primarily through evaporation but also transpiration, infiltration, and runoff processes (Fig. A2). Assigning the sectoral consumption flux directly to the evaporation flux, as done in GHMs, is not a suitable option for CLM5. Owing to the strict requirements for water and energy conservation in CLM5 for coupled applications, transforming the consumed water into evaporation would require updating the surface energy partitioning accordingly. However, by applying the consumption flux to surface soil in naturally vegetated areas, this water can evaporate or not, depending on energy availability, contributing to the surface water–energy exchange. It should be mentioned here that the total consumed flux is not applied to surface soil all at once but dribbled out evenly during the modelled day. This is in contrast to irrigation, where the total withdrawal is distributed uniformly over a period of 4 h, starting with 06:00 local time.

2.3 Input data

The new module for sectoral abstractions relies on input data for all sectors, except irrigation. Data on sectoral withdrawal and consumption are sourced from Huang et al. (2018). This dataset represents a historical reconstruction, which is generated by combining the U.S. Geological Survey (USGS) and the Liu et al. (2016) improved Food and Agriculture Organization of the United Nations (FAO) AQUASTAT dataset on sectoral water use. It covers the period 1971–2010, and it is available on a regular $0.5 \times 0.5^{\circ}$ grid and monthly frequency. The represented sectors are domestic, livestock, thermoelectric, manufacturing, and mining. Irrigation is also represented, but we ignore it here as we use the CLM5's built-in irrigation module.

Domestic water withdrawal encompasses the use of water for various indoor household activities, including drinking, food preparation, bathing, laundry, dishwashing, and toilet flushing. It also includes outdoor uses like watering lawns and gardens, as well as water use by the public sector and service industry. Electricity water withdrawal refers to the water used for cooling thermoelectric and nuclear power plants. Water withdrawal for mining is utilized in the extraction of minerals, which can be solids (like coal), liquids, or gases (such as natural gas). In manufacturing, water withdrawal serves multiple purposes, including fabricating, processing, washing, cooling, or transporting products; incorporating water into products; and meeting the sanitation needs within the manufacturing facilities. These sectoral water withdrawal categories are consistent with the work of Liu et al. (2016) and described in Huang et al. (2018).

To get the final monthly gridded dataset, Huang et al. (2018) used a three-step approach involving spatially downscaling the original country (or state) level data to the $0.5 \times 0.5^{\circ}$ grid level, followed by linear interpolation on the individual grid cell's time series to get the annual sectoral withdrawal from the 5-year interval from the reports, and, ultimately, using a sector-dependent temporal downscaling procedure to go from an annual to a monthly frequency.

For spatial downscaling, Huang et al. (2018) used global population density maps from the History Database of the Global Environment (HYDE; 1970–1980) and Gridded Population of the World (GPW; 1990–2010) for the domestic, thermoelectric, manufacturing, and mining sectors, while using the 2005 FAO global livestock density maps for the livestock sector, following the approach of Hejazi et al. (2014). A uniform distribution is adopted by Huang et al. (2018) for the temporal downscaling of water withdrawal of livestock, mining, and manufacturing. For the domestic sector, a temporal downscaling based on the approach of Wada et al. (2011b) is used, where a modulating function is applied based on each grid cell's historical temperature ranges and a region-dependent amplitude parameter, R (Huang et al., 2018). Finally, the thermoelectric water withdrawal is temporally downscaled using the assumption that thermoelectric

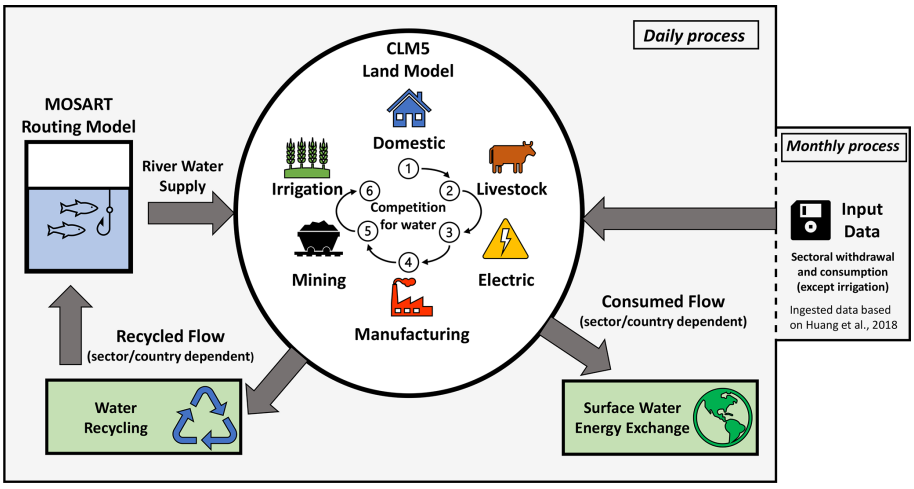

Figure 1. Schematic depiction of the new sectoral water use module implementation in the Community Land Model (CLM5) and the Model for Scale Adaptive River Transport (MOSART).

water use is proportional to the generated electricity, which is then estimated using heating degree days (HDDs) and cooling degree days (CDDs) as proxies (Voisin et al., 2013; Hejazi et al., 2015). The temporal downscaling algorithms for both domestic and thermoelectric sectors were validated and calibrated by Huang et al. (2018), based on existing observations.

The main idea of the Huang et al. (2018) dataset is to represent a reference for historical water use by being derived as much as possible from existing observation/reported data. While the usage of such reconstruction is of interest for historical applications, the new module for sectoral abstractions can accommodate alternative datasets for both historical and future periods, which may be interesting for exploring the uncertainties related to the modelling of human water use and projecting its impact on water scarcity (Wada et al., 2016).

2.4 Understanding the algorithm through a hypothetical case study

To gain a comprehensive understanding of the sectoral water use module, we explore a hypothetical single-grid-cell case study (Fig. 2). In this scenario, we track the dynamics between expected and actual withdrawal during a Northern Hemisphere summer season (June–August, JJA) for a hypothetical grid cell.

As detailed in Sect. 2.2, the model ingests gridded expected withdrawal and consumption data on a monthly basis (Fig. 1). From this monthly expected withdrawal, assuming uniform distribution, we compute the daily expected sectoral abstraction, which remains constant throughout a given month (Fig. 2a).

Certain sectors may exhibit a sudden increase or decrease in the expected withdrawal amount at the onset of a new month. This factor is influenced by the sector and the assumptions which went into the input data. For instance, for the domestic and thermoelectric sectors, the seasonality of the withdrawal in Huang et al. (2018) is modelled by executing temporal downscaling on the annual amounts using monthly surface temperature, as well as heating and cooling days, as a proxy. Conversely, other sectors may show no seasonality (Fig. 2c) due to the absence of strong dependencies (e.g. manufacturing) or because known dependencies such as livestock that increased water requirements during heat waves (Steinfeld et al., 2006) and are not represented in the input data (Huang et al., 2018).

The spatial patterns of water use should also be considered, as they emerge from the utilization of various proxies for spatial downscaling. Some examples include population densities for domestic needs (Wada et al., 2011a; Hanasaki et al., 2018), nighttime light intensity for industrial needs (Droppers et al., 2020), density maps for livestock (Khan et al., 2023), power plant locations for thermoelectric sites (Flörke et al., 2013), and irrigation areas (Burek et al., 2020; Müller Schmied et al., 2021). The selection of proxies used for downscaling, the sectors modelled, and the spatial resolution all influence the mix of sectors that may be represented in a given grid cell. In our hypothetical case study, mining and irrigation are not represented because we assume that no abstraction happens for these sectors in our hypothetical grid cell (Fig. 2f).

As explained in Sect. 2.2, CLM5 and MOSART can exchange the information on local water availability at the beginning of each day and adjust the actual sectoral abstractions while considering the sectoral priority. In our example, we assume that a small local water deficit occurs in June, satisfying high-priority sectors like domestic and livestock fully, while the thermoelectric sector experiences a supply gap (Fig. 2d). While the sector higher in priority (thermo-

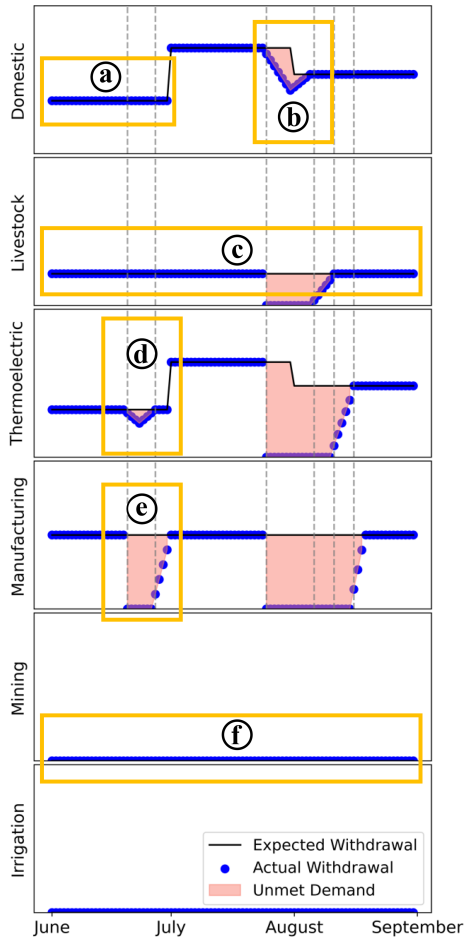

Figure 2. Illustration of potential outputs from the sectoral water use module for a hypothetical single-grid-cell case study. The sectors are arranged by order of priority from top to bottom. The figure elucidates the interplay between expected (input-based) and actual (taking into account limited availability) sectoral water withdrawals under both normal and water stress conditions. Factors such as river water availability and inter-sector competition, as previously outlined (Fig. 1), are integral to this model's function and results. Each labelled box represents a feature of the algorithm/model, which is discussed in Sect. 2.4. In addition, the interrupted vertical lines help identify the moments when water scarcity begins for a given sector and how the supply gradually recovers by order of priority.

electric) is not satisfied fully, no abstraction is happening for the sectors lower in priority (manufacturing; Fig. 2e).

Similarly, we suppose a larger water deficit in July–August that affects the domestic demand directly (Fig. 2b). As a consequence, the other sectors only recover when the sector higher in priority is fully satisfied. While the scarcity and recovery processes are represented in this example with linear trends, these patterns are noisier in the model, following the day-to-day water balance dominated by precipitation, evapotranspiration, and runoff processes.

2.5 Experimental setup

CLM5 simulations are conducted for the period between 1971 and 2010, with the first 2 years excluded for spin-up (the analysis period is thus from 1973–2010). Two simulations were conducted: a control simulation without sectoral abstractions and without irrigation, referred to as CTRL, and another simulation with complete sectoral water abstractions, including irrigation and the five new sectors, referred to as SectorWater.

Both simulations used a scientifically validated configuration designed for land-only simulations (IHISTCLM50BgcCrop component set). This configuration captures the historical changes in climate, CO_2 levels, and transient land use and land cover change, including cropland expansion; it uses the Global Soil Wetness Project atmospheric forcing dataset (GSWP3v1), models terrestrial biogeochemical cycles, and includes a prognostic crop model (Lawrence et al., 2019). The simulations were run with a horizontal resolution of $0.9 \times 1.25°$ and a default 30 min time step. While it would have been possible to run simulations at higher resolutions (e.g. $0.5 \times 0.5°$), we opted for the $0.9 \times 1.25°$ grid because it is one of the two scientifically supported grids for the IHISTCLM50BgcCrop configuration. In future applications, where the focus extends beyond demonstrating the module's capabilities, a higher-resolution setup may be preferred to provide more detailed regional insights.

Here we showcase the new module capabilities using land-only simulations. While testing the module in fully coupled CESM simulations is outside the scope of this study, this development is fully compatible with such applications.

3 Results

3.1 Testing and validation

Since we rely on a data-driven approach, and the input data we are using are from an evaluated reconstruction of historical water use (Huang et al., 2018), our validation focuses on the reliability and robustness of the implementation itself.

Initial tests focus on ensuring data consistency by verifying the robustness of remapping of the original sectoral water use dataset from $0.5 \times 0.5°$ to $0.9 \times 1.25°$ on the CLM5 land mask. In general, the remapping procedure is found to be conservative (Fig. B1), with relative errors of about 1 %–2 % explained by upscaling effects when passing to a lower-resolution land mask (Fig. B2).

To verify the correct behaviour, we compared expected and actual model-based sectoral abstraction fluxes with the input data. We confirm that expected fluxes at the grid cell level match the input data, while actual fluxes are always lower than or equal to the expected fluxes when grid cell river networks lack sufficient water (Figs. B3–B4). The sector priority algorithm was confirmed to function correctly,

with no lower-priority abstractions occurring when higher-priority sectors are unsatisfied (Fig. B5).

Next, the successful coupling between the land and the routing models is verified (Sect. 2.2). It was confirmed that the fluxes from the land model match the fluxes from the routing model at both global and continental level (relative errors $< 1\,\%$; Taranu, 2024a), demonstrating that the differences in resolution and spatial organization were taken into account during both the coupling process and the two-way remapping of the sectoral abstraction fluxes from land to the river network. While maintaining the same spatial patterns, the map corresponding to the MOSART output (Fig. 3b) has more details and sometimes more pronounced local values. This is because MOSART operates at a higher resolution in this case ($0.5 \times 0.5°$ versus $0.9 \times 1.25°$ for CLM5) and has a different spatial organization with main channels of different storage. As a consequence, the sectoral fluxes from the CLM5 grid cell may be remapped unequally between MOSART's intersecting grid cells (see Sect. 2.2 for a detailed description of the coupling process).

Finally, CLM5 ensures mass and energy conservation by aborting the simulation when this is violated.

3.2 Historical trends in global sectoral withdrawal

Over the period 1973–2010 (Fig. 4), sectoral water withdrawals show mostly a steady increase, followed by a slight decline towards 2010. While irrigation is consistently the largest contributor, other sectors account for a substantial share, especially looking at the actual withdrawal. By 2010, the cumulated non-irrigative expected sectoral withdrawal and consumption reached 1157 and $171\,km^3\,yr^{-1}$, respectively, which represent an increase of $315\,km^3\,yr^{-1}$ or 36 % for the period 1971–2010. The total global expected and actual water withdrawal increased by 110 % and 43 %, respectively. Over the same period, in the SectorWater simulation, the expected (actual) irrigation withdrawal accounts for 79 % (36 %) of the total water withdrawal, followed by domestic with 6 % (19 %), thermoelectric with 8 % (23 %), manufacturing with 5 % (14 %), and, finally, livestock and mining together with about 2 % (8 %).

Comparing the results on the relative importance of each sector with the results from Huang et al. (2018) reveals that the mean relative importance of irrigation is substantially higher in our case (79 % versus 68 %). To comprehend the findings of the SectorWater simulation, it is essential to consider two key factors. First, CLM5 computes irrigation water requirements prognostically by taking into account the soil moisture deficit for each day which needs to be covered to satisfy crop water requirements. At the same time, in some regions, CLM5 struggles to supply enough water for irrigation using river water alone (Fig. E6). When analysed globally, based on the SectorWater experiment results, CLM5 supplies only 10 %–20 % of what is globally requested (Fig. C1d), compared to $> 96\,\%$ for all the other sectors. But this difference in supply should be interpreted cautiously. Due to the lack of water supply in certain areas, soil moisture levels are frequently below optimal levels. This results in a consistent water deficit for crops, leading to a greater reliance on irrigation. Consequently, this increases the overall annual expected irrigation withdrawals globally, which are likely exaggerated in our experiment.

In fact, when only irrigation is considered, and no limit on water supply is imposed, CLM5 underestimates the total irrigation withdrawal in comparison to other models or AQUASTAT estimates. For example, in CLM5 it is possible to overcome the limitation of river water availability for irrigation supply through a negative subsurface runoff term in the MOSART model, which is then compensated with ocean water. This is an unrealistic configuration, but at the moment it is required to close the water balance when supplying the full irrigation requirements. It is also interesting to use when studying the land–atmosphere interactions and feedbacks of irrigation when the total withdrawal rather than the impact on discharge and runoff is important (Thiery et al., 2017; Chen and Dirmeyer, 2019; De Hertog et al., 2023). In this configuration, and using a similar version of the model as in our study, Yao et al. (2022) found that the mean expected global irrigation water withdrawal for the period 1981–2015 is about $910\,km^3\,yr^{-1}$. This is largely below the range given by the other models of about $2000–4000\,km^3\,yr^{-1}$ for the same period (McDermid et al., 2023) and significantly lower than the expected irrigation withdrawal in our SectorWater experiment. Using the Yao et al. (2022) estimates for expected withdrawal, it seems that using river water alone could satisfy up to 50 % (vs. the 10 %–20 % estimated based on our results) of the current CLM5 irrigation requirements (Fig. 4b). In this context, an analysis by the sector of the fractions of unmet demands during the 1981–2010 period reveals that the global shortfall in irrigation supply is not due to competition with recently introduced sectors. This conclusion is supported by numerous grid cells, where only the irrigation sector exhibits undersupply (Figs. E1–E6).

This low estimate of global irrigation water withdrawal ($910\,km^3\,yr^{-1}$ vs. $2000–4000\,km^3\,yr^{-1}$) could be a consequence of the fact that the default irrigation technique used for all crops in CLM5 is very efficient and akin to drip irrigation. By introducing different irrigation techniques, including drip, sprinkler, and flood, as well as a special parameterization for rice paddies, Yao et al. (2022) were able to reduce the bias in irrigation withdrawal compared to observations; this increased the total global irrigation withdrawal to about $3600\,km^3\,yr^{-1}$. Vanderkelen et al. (2022) also suggested that CLM5 is likely underestimating irrigation totals, as well as irrigation seasonality, based on independent comparisons of reservoir inflows with observed values. Taking these results into account, and anticipating larger expected irrigation withdrawals in future versions of CLM5 in line with observations and improved irrigation representation, it becomes critical that the water supply parameterization within CLM5 gets

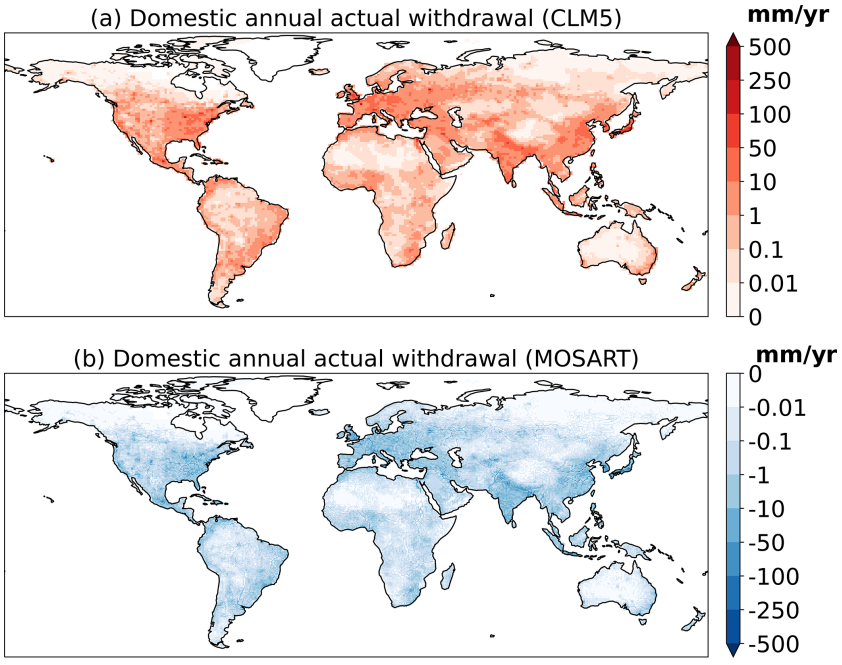

Figure 3. Actual domestic withdrawal for the year 2000 as outputted by the CLM5 **(a)** and MOSART **(b)** components. Sectoral withdrawal is a positive term for the land component, which gains water from consumption, and a negative term for the routing component, which loses water (Fig. 1).

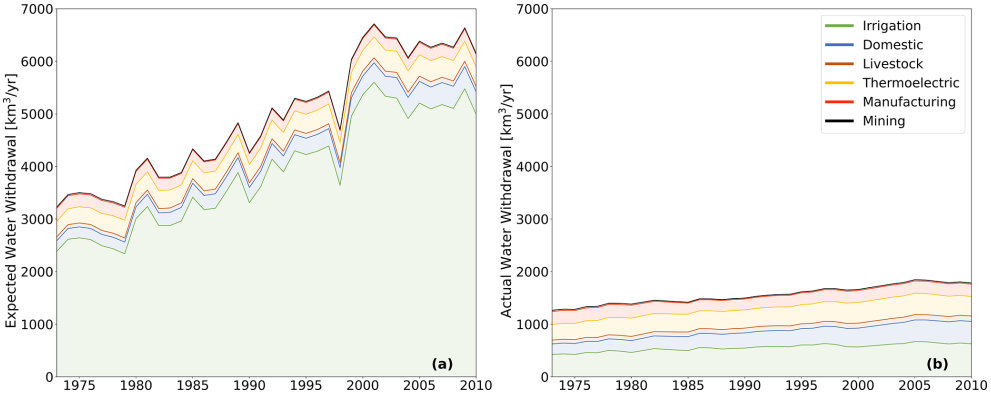

Figure 4. Annual global expected **(a)** and actual **(b)** sectoral withdrawal throughout the years 1973–2010. The actual withdrawal volumes can be lower than the expected ones because of limited river water availability and sectoral competition for limited resources (Figs. 1 and 2 for details). This figure was produced using the SectorWater experiment results. The trends and fluctuations in the expected irrigation withdrawal time series are due to the changes in climate and historical cropland expansion, both captured in the SectorWater experiment (see Sect. 2.5 for a description of the experimental setup).

improved. This includes the implementation of abstractions from renewable and fossil groundwater, as well as from lakes and reservoirs.

3.3 Regional patterns in sectoral water use

Spatial patterns in sectoral water use vary significantly by region, influenced by climate, economic activities, and population distribution (Fig. 5). In areas experiencing precipitation deficits or with intensive agricultural activities, like the western US, eastern China, and the Indo-Gangetic Plain, irrigation demands are the highest (Jägermeyr et al., 2015; Huang et al., 2018). High sectoral water use aligns in general with the local density of the population, but there are also exceptions based on regional characteristics such as economic activities, climate, or water availability (e.g. dominance in the eastern US of thermoelectric water usage of the country).

Different socio-economic and climatic conditions lead to diverse water use profiles (see the map in Fig. 6). Agriculture-dominated water use is prevalent in many

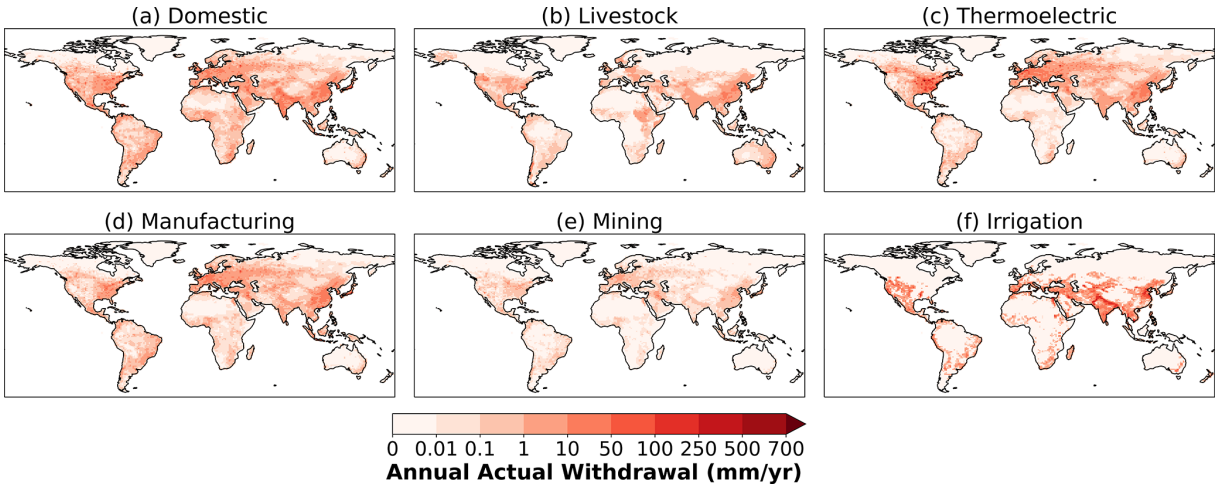

Figure 5. Spatial distribution of actual sectoral withdrawal for the year 2010 as outputted by the CLM5 land model in the SectorWater simulation. Note that the colour bar is non-linear.

African, Asian, and South American countries, whereas industrialized nations in Europe and North America show a greater emphasis on industrial water use. Arid regions like the Middle East have higher domestic and agricultural water use due to increasing population and urbanization, while the high evapotranspiration rates and limited soil moisture make irrigation essential for crop growth (World Bank, 2017).

From 1973 to 2010, water withdrawal trends changed, reflecting socio-economic progression, population dynamics, and changes in regional climate (see the time series subplots in Fig. 6).

In East Asia and South Asia, there has been a notable rise in irrigation water use. This increase is likely attributed to warmer temperatures and expanding agricultural land for a growing population (Lombardozzi et al., 2020), both of which are captured by the SectorWater simulation (see Sect. 2.5 for more details).

Most of the Global South regions experience a significant increase in their domestic and industrial water usage, likely a consequence of the increasing population, rapid urbanization, and economic development (Wada et al., 2011a). At the same time, industrial water withdrawal in North America and Western Europe has stabilized or declined, potentially due to technological advances and economic shifts leading to higher water use efficiency (Flörke et al., 2013). Eastern Europe and central Asia exhibit similar patterns but are likely influenced by post-Soviet-era transitions (Kummu et al., 2016).

Livestock water demand trends vary, with significant increases in North America, South America, and South Asia, following dietary changes and increasing global protein requirements (Rust, 2019). Some regions, however, have stabilized or decreased livestock water use, suggesting advancements in livestock production systems (Rust, 2019).

3.4 Impact on the climate

Irrigation withdrawal shows the strongest correlation with the regional climate differences when compared to other sectors' cumulative consumption (Fig. 8). A linear regression analysis gives $R^2 \approx 0.9$ for irrigation withdrawal vs. $R^2 \approx 0.08$ for other sectors' consumption to explain the climatic variable differences between the CTRL and SectorWater experiments (Fig. 7 a, c, e). There are a few reasons why we do not find a significant effect for the non-irrigative sectoral consumption on the selected surface variables in our experiment. For example, for non-irrigative sectors, the cumulative consumption is quite small; it is distributed over the year and the entire day (24 h) and independently of soil moisture conditions, and it is distributed over a larger area (natural vegetation column). As a consequence, the impact of non-irrigative sectors on the climate is insignificant at scales of a 100 km and above. For irrigation, the water is applied for parts of the year when the crops grow and only when there is a moisture deficit. Moreover, the irrigation window is short and applied over 4 h at 06:00 local time. In addition, the water is locally applied over the columns with irrigated crops, and the total irrigation amounts are very large (e.g. maximum cumulative grid cell consumption for non-irrigative sectors is only at the low end of the irrigation grid cell withdrawal in Fig. 7). These conditions ensure that irrigation will have a significant impact on the local climate, since a significant amount of water is provided locally over a short period of time in a moment when evaporation and plant transpiration is limited by water availability.

These findings underscore irrigation's principal role as a climate forcing in relation to human water use (McDermid et al., 2023), with the contribution of other sectors being negligible at a large scale. Despite this, incorporating other sectors' abstractions into Earth system models (ESMs), as sug-

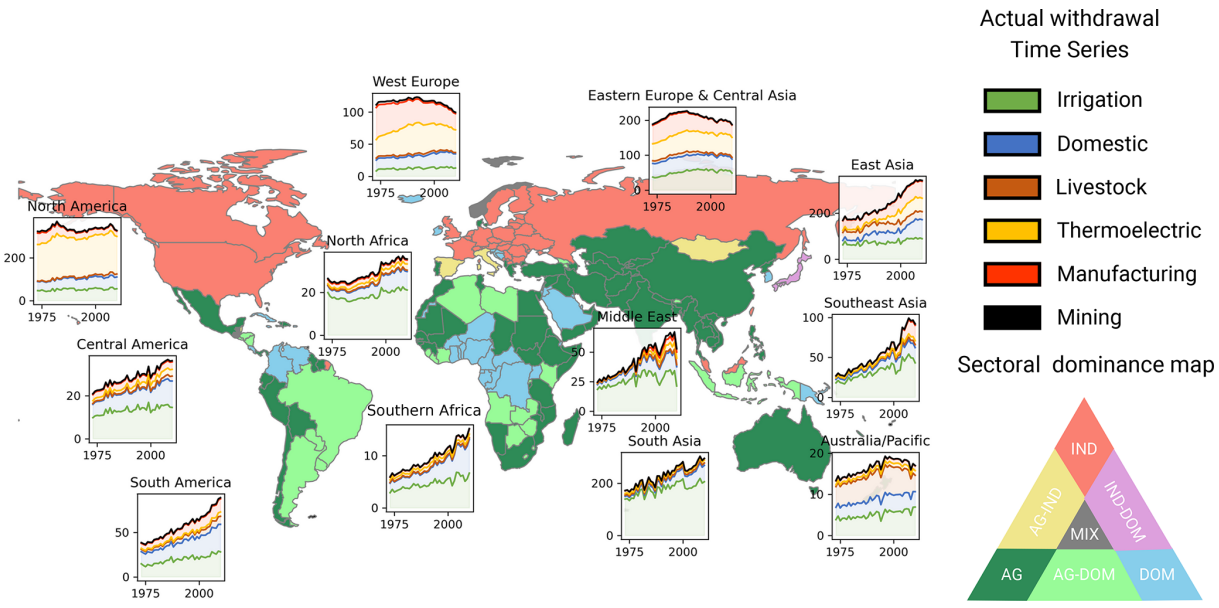

Figure 6. Classification of countries based on their dominant sectoral water use as sourced from mean actual withdrawals for six sectors (irrigation, domestic, livestock, thermoelectric, manufacturing, and mining) between 1973 and 2010. For clarity, irrigation and livestock data were combined under "agriculture" (AG), while thermoelectric, manufacturing, and mining were aggregated as "industry" (IND), and domestic is considered separately (DOM). A sector is dominant when it accounts for over 50 % of the total mean withdrawal throughout the observed period 1973–2010 (e.g. AG). A mixed usage is when no sector accounts for more than 40 % or less than 30 % of the mean total withdrawal, indicating an even distribution across sectors (MIX). Dual dominance is when leading sectors together represent more than 65 % of total mean withdrawal, with neither falling below 25 % (e.g. IND–DOM). The dominance map format is inspired by a similar map presented by World Resources People and Ecosystems (2000). Accompanying the map are time series plots detailing actual withdrawals for the 12 major geographical regions.

gested by Nazemi and Wheater (2015), remains important for evaluating water scarcity in present and future climates, as well as the changes in surface and groundwater storage resulting from sectoral withdrawal and consumption. For example, comparing the SectorWater and CTRL experiments shows a significant decrease in mean annual streamflows for most major rivers (Fig. D1), as well as a decrease in total annual river discharge to the ocean of about 300 $km^3\,yr^{-1}$ by the year 2010 (Fig. D2).

3.5 Water scarcity

By visualizing the average number of days when the local supply of surface water was not sufficient to fully satisfy all sectoral demand (Fig. 9), we find that the results produced by the updated CLM5 closely match known hotspots of water scarcity (Mekonnen and Hoekstra, 2016; Kummu et al., 2016; Liu et al., 2017).

Analysing model results, we find that the largest regional water scarcity is found in the Middle East. For example, by aggregating results at sub-national level (Fig. E7), we find that the municipality of Al Khor, Qatar, experiences water-scarce conditions for about 320 d per year on average, where local river water is not enough to fully satisfy its residents' demands. Other known hotspots of water scarcity in the Middle East (World Bank, 2017) are well captured by the model, including Haifa in Israel (195 d), the West Bank in Palestine (140 d), Daraa in Syria (125 d), Jizan in Saudi Arabia, Sharjah and Dubai in the United Arab Emirates (about 90 d), and Amran and Raymah in Yemen (about 150 d). The reasons are multifaceted, ranging from climatic challenges, with prolonged droughts and erratic rainfall, to increasing populations and standards of living accompanied by increasing domestic and agricultural demands (Fig. 6). To manage these challenges, the region heavily depends on fossil groundwater exploitation, leading to rapid groundwater depletion (World Bank, 2017; Bierkens and Wada, 2019). As a result, the region is making substantial efforts to find alternative sources of water, such as through desalination (Eke et al., 2020; Curto et al., 2021).

The Mediterranean, another region historically vulnerable to water stress, presents a similar narrative. Spain's Region of Murcia and Andalucia or Greece's Crete, all with over 100 d of unmet water demand in our simulations, are typical of the region, grappling with both climatic adversities and high agricultural demands. Climate change is expected to further intensify this issue, with projections indicating reduced rainfall and soil moisture in the region (Fig. TS.5 in Arias et al., 2021).

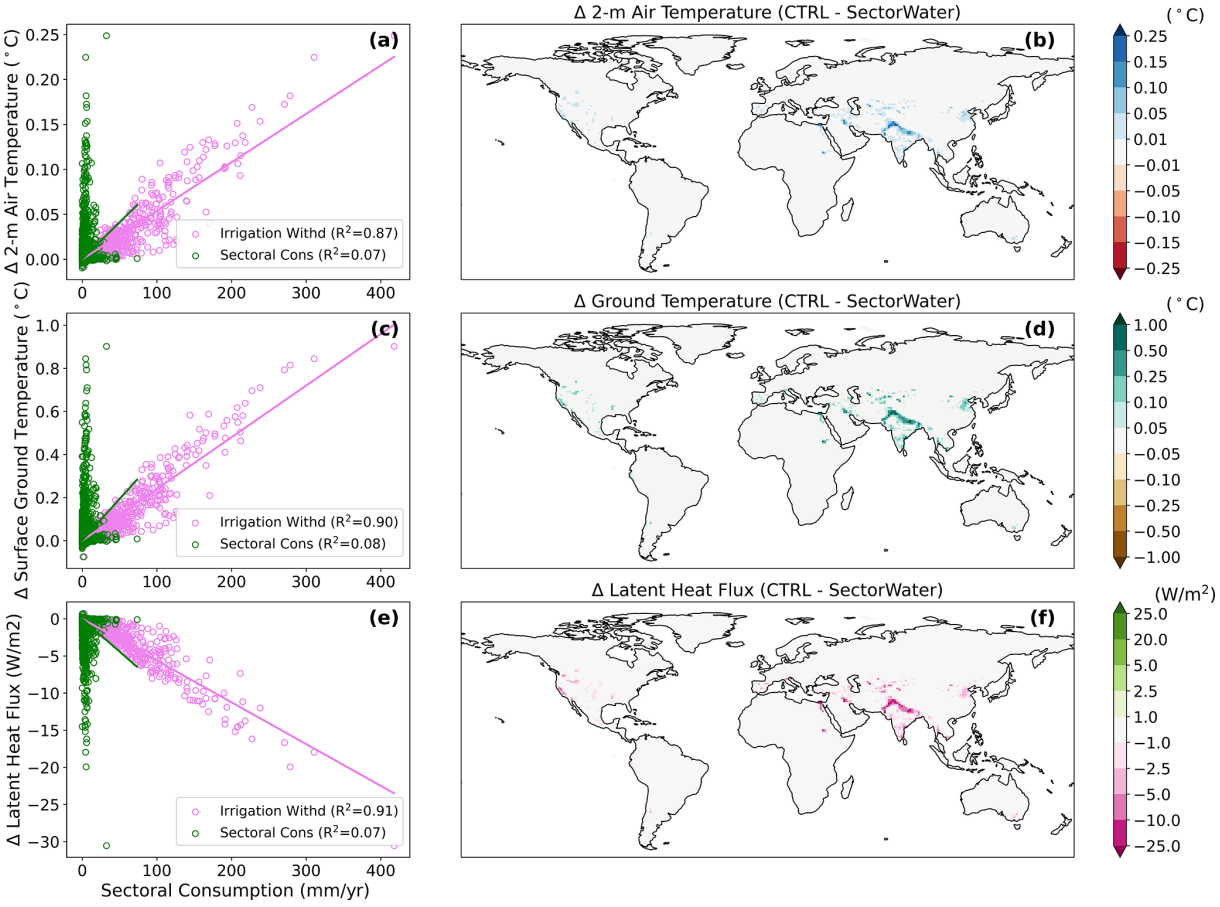

Figure 7. (b, d, f) Mean difference maps for 2 m air temperature, ground temperature, and latent heat flux between the CTRL and SectorWater experiments. The maps are generated by calculating the difference between each month for the given variable between the years 1973–2010 and then computing the average over all the differences. **(a, c, e)** Linear regressions between the difference maps for the given variable and one of the predictors, i.e. the mean irrigation withdrawal or the mean sectoral consumption (see predictor maps in Fig. 8). Each point in the regression plots represents individual grid cells from the corresponding right-hand-side difference map.

Turning to Asia, the model results resonate with well-documented concerns. Regions in India, such as Karnataka and Maharashtra (about 120 d), and areas in China, like Tianjin and Hebei (about 60 d), are well known for water scarcity. For example, previous studies showed water stress that ranges between 40 %–80 % in the Karnataka and Maharashtra region (Manju and Sagar, 2017), while water supply for the Beijing–Tianjin–Hebei urban agglomeration represents a significant challenge requiring trade-offs among economic development, environmental protection, and nexus risks in the adjacent regions (Cai et al., 2021). In central Asia, the Sughd Province in Tajikistan stands out with 100 d of unmet demands. This region is known for high overall water scarcity, especially during peak irrigation seasons, leading to strong competition over water resources and a local practice of water rotation to ensure supply (Mukhamedova and Wegerich, 2018).

When it comes to North America, the region which stands out the most in our simulations is the state of California (60 d). With over 8.5 million acres (3.5 Mha) of irrigated cropland, the state of California is vulnerable to frequent and intensifying droughts and tends to rely on unsustainable groundwater exploitation (Mount and Hanak, 2019). This led to the adoption of the 2014 Sustainable Groundwater Management Act which requires pumpers to reach sustainability by the early 2040s. At the same time, the model seems to capture the continuing difficulties in Colorado (25 d). Between the period from 1916–2014, the Upper Colorado River basin experienced a 16.5 % decline in naturalized streamflow, which is met by increasing population and sectoral demand often being equal to the inflows (Xiao et al., 2018). For these reasons, and general low groundwater availability, the Colorado basin is one of the basins with the highest projected economic impact uncertainty in the world in future climate scenarios (Dolan et al., 2021).

Other water scarcity hotspots which seem to be captured by the model are western South America, southern Africa,

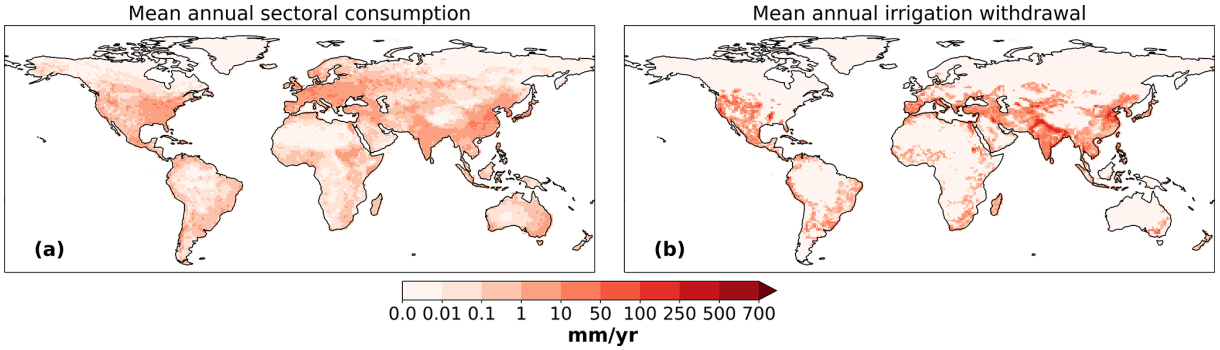

Figure 8. Spatial distribution of mean annual consumption for all sectors (excluding irrigation) alongside annual irrigation withdrawal, both used as predictors in the regression depicted in Fig. 7. It can be noted that irrigation withdrawal correlates much better with the surface climate variables in Fig. 7. While the irrigation withdrawal is in general much larger than non-irrigative sectoral consumption, this is especially the case for the grid cells where a climate-modulating effect is observed (Fig. 7).

northwestern Africa, and southeast Australia, in line with previous research (Mancosu et al., 2015; Liu et al., 2017).

To better understand individual contributions, we analyse the same metric for individual sectors (Fig. 10). We note that irrigation is by far the largest contributor to water scarcity, in terms of both the spatial extent and intensity. At the same time, we are observing a significant number of days with unmet demands for the other sectors too in regions known to have difficulties with water supply. The regions which stand out for non-irrigative water scarcity are Al Khor and Al Wakrah in Qatar, Toa Alta in Puerto Rico, Haifa in Israel, Al Marqab in Libya, Istanbul in the Republic of Türkiye, the West Bank in Palestine, Al Ismailia in Egypt, Makkah in Saudi Arabia, and Tehran and Isfahan in Iran. As can be seen, the regions affected by non-irrigative water scarcity, in our analysis, are mostly located in the densely populated regions of the Middle East, the Mediterranean, India, western North America, and northern Africa. Due to the implemented prioritization order (see details in Sect. 2.4), we can see a cascading effect, with the intensification of existing unmet demands and new regions being affected for each new sector down the priority order. These results are likely to change significantly, depending on the allocation order, representing an important uncertainty for the individual sector's water scarcity assessments (Rathore et al., 2024). The complete analysis for each country at a sub-national level can be found in the associated data repository.

We find that for the period from 1973–2010, a general trend of the intensification of water scarcity is observed for most of the affected countries. This is expressed in an increasing fraction of the country struggling with sectoral water supply (e.g. India, Qatar, or Saudi Arabia in Fig. 11) or an increasing number of days per year during which the affected regions are exposed to such conditions (Fig. 12). For some countries, we have seen the emergence of unmet sectoral demands (especially for non-irrigative sectors) only relatively recently (e.g. years from 2000 onwards for Brazil, China, Pakistan, and Turkmenistan in Fig. 11). There are also situations in which unmet sectoral demands become less common (e.g. Russia in Fig. 11). In most cases, the observed long-term trends in the historical water scarcity can be explained by changes in countries' sectoral demands (Fig. 13). With increasing sectoral water needs, many regions have reached or are over their surface water availability limit (Wada, 2016). At the same time, there are also some exceptions which cannot be explained simply by changes in sectoral demands (e.g. the drop in domestic/livestock water supply in the US between the 1980s and 1990s or the drop between the 1990s and 2000s in Saudi Arabia for all sectors' supply). This indicates the existence of some other sources of water scarcity, such as long-term natural variability (Rodell et al., 2018). But in this study, we do not aim at disentangling the exact reasons for unmet demands between natural variability, climate change, and changes in sectoral demands.

4 Limitations and a way forward

While our additions to CLM5 represent a notable advancement in the representation of human water use in the Community Earth System Model (CESM), there are still some limitations and assumptions that should be acknowledged.

In the latest iteration of the CLM5, an alternative mechanism allows for the extraction of unmet water demand for irrigation from unconfined groundwater in addition to the supply from the rivers (confined aquifers are currently not supported by the model). This approach provides a more realistic depiction; however, a potential limitation is its exclusive reliance on model-calculated renewable groundwater availability. Given the present model's omission of water abstractions from reservoirs and lakes, there is a likelihood of overestimating groundwater dependence in certain areas. Conversely, there is the potential for a significant underestimation of groundwater abstractions in arid and semi-arid regions. These regions often experience minimal groundwater

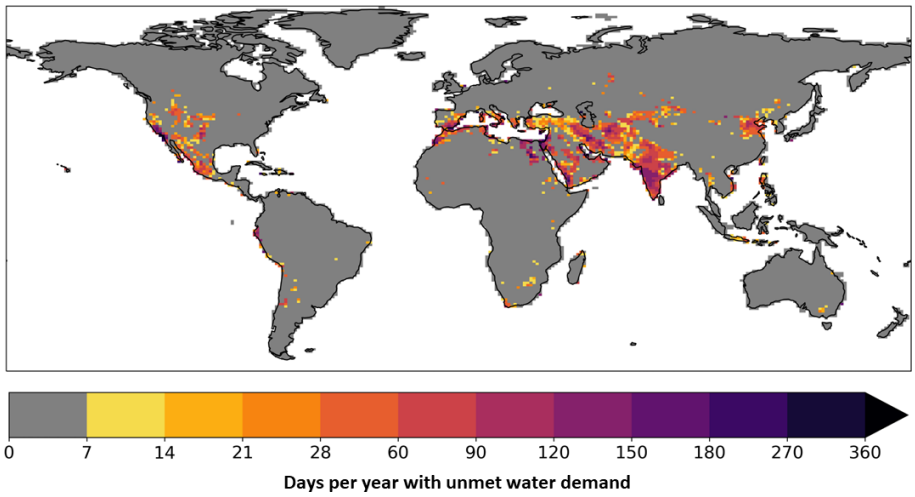

Figure 9. Average number of days per year, from 1973–2010, when modelled water supply was insufficient to meet the demand for all sectors. Note the non-linear colour bar.

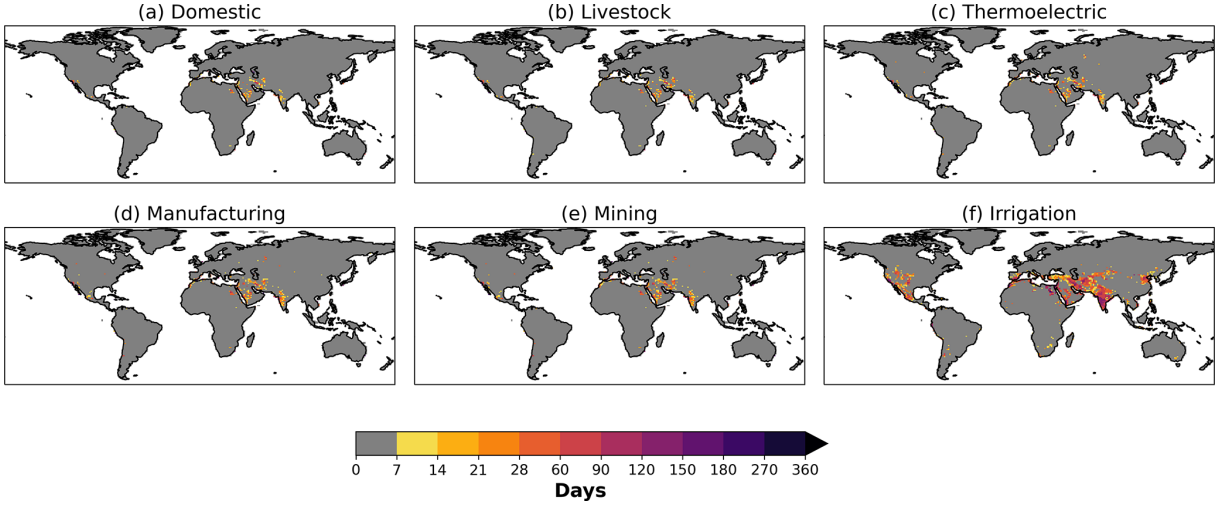

Figure 10. Average number of days per year, from 1973–2010, when modelled water supply was insufficient to meet the demand for individual sectors. Note the non-linear colour bar.

recharge (Bierkens and Wada, 2019), and the model currently does not account for fossil groundwater reserves. Nevertheless, comprehensively accounting for every source of sectoral water withdrawal is crucial for the valid application of CLM5 in water scarcity assessments. Therefore, evaluating the efficacy of this new groundwater abstraction approach, along with its expansion to recently incorporated sectors, emerges as an imperative future effort.

In the context of groundwater abstractions, it is also important to consider how the partitioning between surface and groundwater dependence is implemented. The method currently available in CLM5 for irrigation is what can be called an implicit method, where the amount supplied from groundwater is based on what remains unsatisfied from surface water (rivers). The advantage of following this approach is that it gives better estimates, especially in regions where significant groundwater pumping remains unreported (Wada, 2016). However, the implicit method may neglect physical, technological, and socio-economic limitations in groundwater use that exist in various countries (Wada, 2016). Alternative methods exist which rely on national and sub-national statistics to calculate the fraction of withdrawal satisfied by the source for each sector (Döll et al., 2012). Such methods are more likely to capture regional/national patterns of groundwater use but may be too conservative due to the problem of unreported usage and a lack of reliable data for many countries (Döll et al., 2012; Wada, 2016). We think that a mixed approach, where the fractions of surface vs. groundwater usage per sector are given but not fixed, may be of interest. With the increased quality and availability of re-

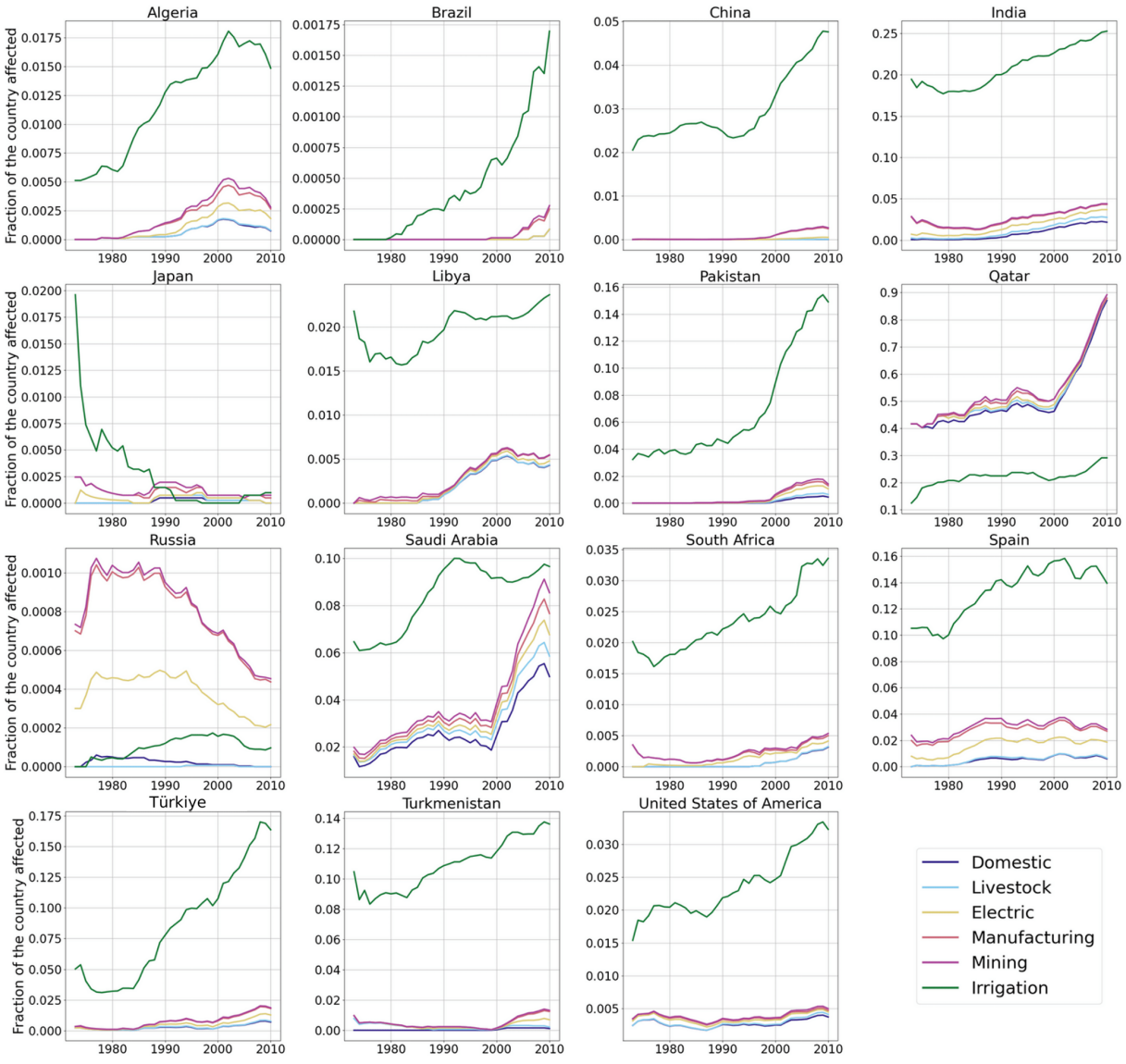

Figure 11. The fraction of the country with at least 1 d per year on which the modelled water supply was insufficient to meet the demand for individual sectors. The results are provided as a 10-year rolling average for a better representation of long-term trends.

mote sensing data, such as GRACE (Gravity Recovery and Climate Experiment), we can imagine using the fractions of surface vs. groundwater usage as a model calibration parameter to better constrain groundwater abstractions using the observed terrestrial water storage (TWS) changes (Anderson et al., 2015; Wada, 2016).

In addition to the implementation of more conventional sources of water supply including rivers, lakes, reservoirs, and groundwater, it may be important to also consider alternative sources such as desalination and treated wastewater (Van Vliet et al., 2021). A recent assessment showed that desalination capacities are increasing globally at an exponential rate, and in 2020 the annual production was at about 35 $km^3\,yr^{-1}$ (Jones et al., 2019). In addition, for the year 2015, wastewater was produced at a rate of about 360 $km^3\,yr^{-1}$ globally, of which only about 10 % was intentionally re-used after treatment (Jones et al., 2021). While these unconventional water sources are still 2 orders of magnitude below the global sectoral withdrawal, they are most often employed in water-scarce regions (Jones et al., 2019, 2021) where they can significantly reduce severe water scarcity and reduce the number of people affected by it (Van Vliet et al., 2021).

Van Vliet et al. (2021) also underscore the significance of the water quality in exacerbating water scarcity. The research reveals that 40 % of the global population faces severe water scarcity when accounting for both water quantity and quality, compared to 30 % when only quantity is considered. In

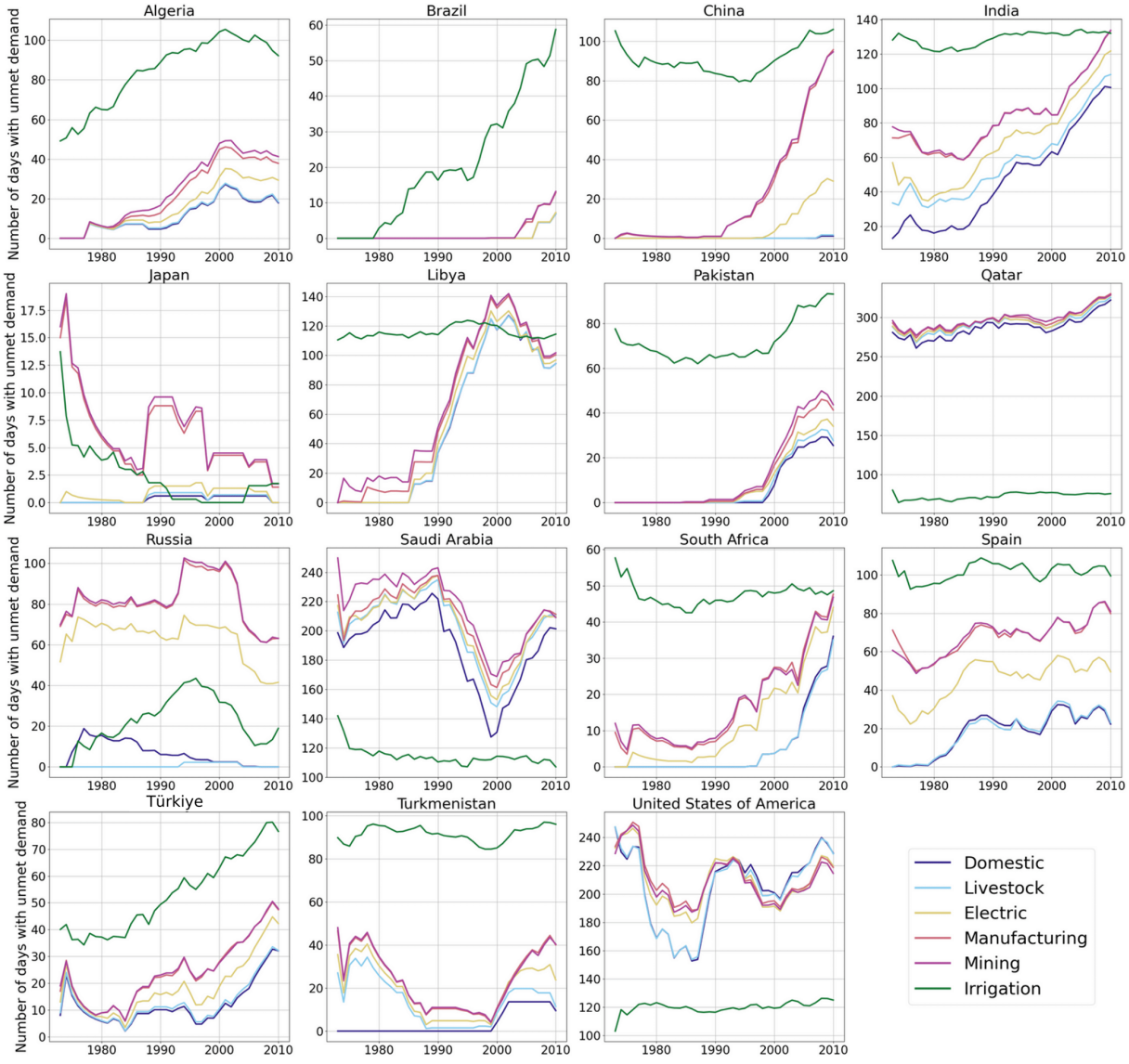

Figure 12. The average number of days per year on which countries are exposed to unsatisfied sectoral demand. The average is calculated only using the grid cells which experience water scarcity conditions. The results are provided as a 10-year rolling average for a better representation of long-term trends.

the future, more GHMs/LSMs may incorporate water quality indicators (e.g. surface water temperature, salinity, organic pollution) in order to provide more precise information on both water quantity and quality. In comparison to GHMs, the LSMs possess the distinct advantage of having a coupling capacity with other components (e.g. ocean and atmosphere) and, often, existing tracing modules (e.g. for tracing isotopes). As such, the development of water quality indicators in LSMs may be easier and have a wider application range (e.g. tracing pollutants in the ocean after discharge). In this context, when developing the sectoral abstraction modules in other GHMs/LSMs, maintaining the withdrawal and return fluxes separately for each sector will be important. While more redundant and computationally more expensive, it allows for an easier implementation of a water quality module in the future by connecting the sector-dependent pollutants (e.g. temperature for thermoelectric or nitrogen and phosphorous pollutants for livestock) to the return flow of each sector (Van Vliet et al., 2021). At the same time, water quality indicators will help calculate sector-dependent extra withdrawals for dilution to obtain acceptable water quality levels for each sector, which thus will improve the water scarcity assessment capabilities of the models (Van Vliet et al., 2021).

The over-abstraction of surface water at the expense of environmental flow is another important aspect of water security that needs to be addressed in the GHM/LSM devel-

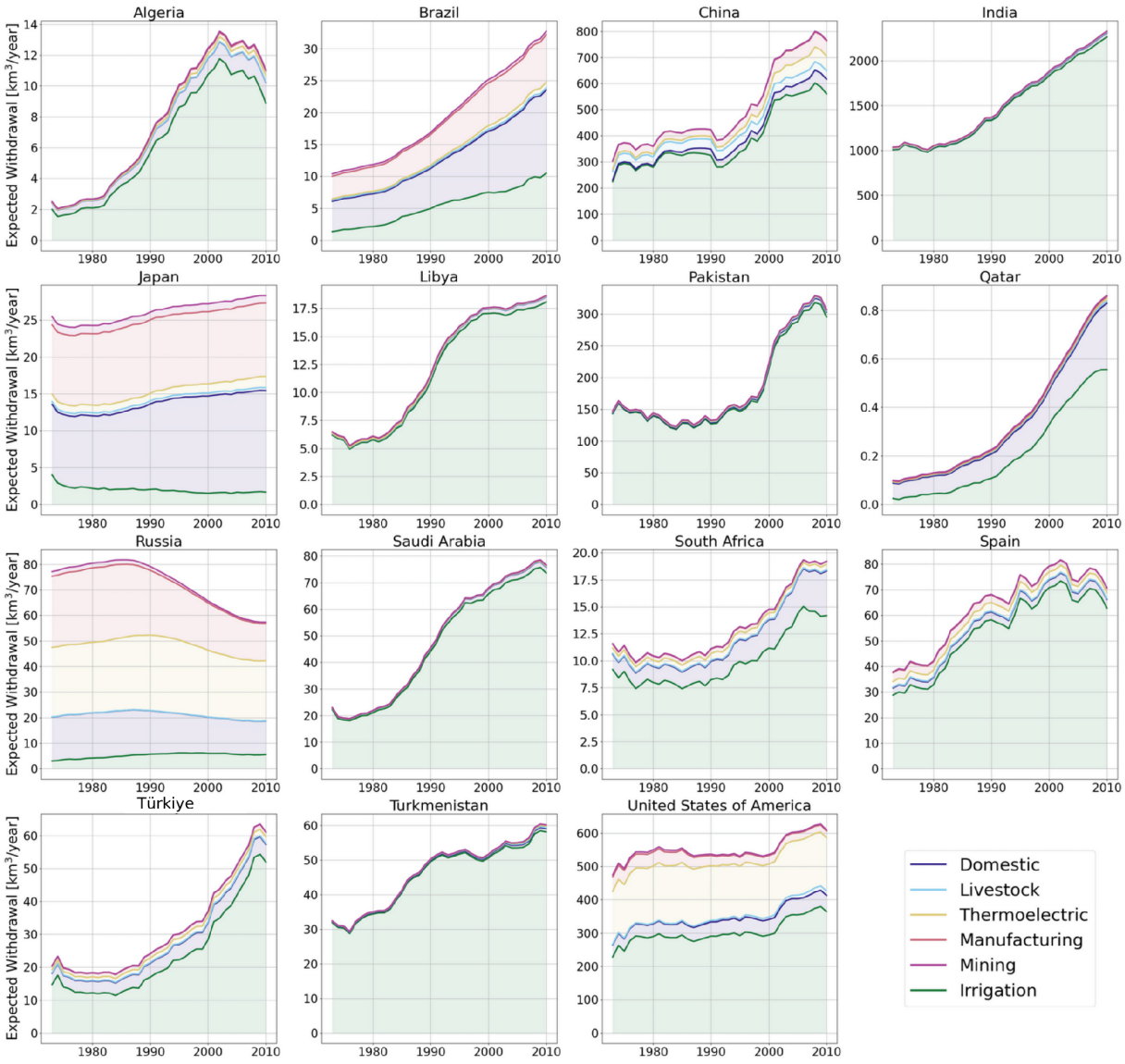

Figure 13. Countries' sectoral withdrawal for the years 1973–2010. The results are provided as a 10-year rolling average for a better representation of long-term trends.

opment. Today, more than a quarter of the surface water consumption in South, West, and central Asia; northeastern China; Spain; and Argentina is considered unsustainable or at the expense of the environment (Wada, 2016). Because of increasing human water use (Wada et al., 2016) and drier climate conditions (Trenberth, 2011), new hotspots of non-sustainable surface water use are emerging in the USA, Mexico, the Mediterranean, the Middle East, and northern and southern Africa (Wada, 2016).

At the moment, the way environmental flow requirements (EFRs) are treated in the CLM5 is by limiting the amount which can be subtracted for sectoral use to 90 % of the current river water availability. This approach allows avoiding the complete depletion of rivers, but it is likely severely overestimating the amount of water which can be abstracted for sectoral use. For example, global assessments have shown that on average, about 37 % of annual discharge is required to sustain EFRs (Pastor et al., 2014). During low-flow periods, the EFRs are even larger and may need 46 %–71 % of the available water (Pastor et al., 2014). In order to improve the capability of CLM5 to account for both human and environmental water needs, the implementation of variable flow-based methods to estimate EFRs is recommended. These methods classify the flow regime into high-, intermediate-, and low-flow months and take into account the intra-annual variability in flow conditions, thus providing better estimates of EFRs under a variety of flow regimes (Pastor et al., 2014).

In our model, sectoral water use priorities are currently fixed and follow the order (in decreasing priority) of domestic, livestock, thermoelectric, manufacturing, mining, and irrigation. While a similar hierarchy was also implemented in some other models (Hanasaki et al., 2018; Droppers et al., 2020), in reality the priority may vary based on regional circumstances, weather, policies, or changing socio-economic conditions. For example, a recent study suggests that in many regions the domestic and irrigation sectors often receive a higher priority than other sectors during periods of droughts, heat waves, and compound hot–dry extremes (Cárdenas Belleza et al., 2023). At the same time, regional exceptions are possible, highlighting the need for more flexible approaches to modelling sectoral competition in GHMs and LSMs (Cárdenas Belleza et al., 2023). For example, a recent study explored an alternative prioritization in which agricultural demands are placed first (Rathore et al., 2024). This scenario resulted in around a 30 % increase in unmet demands for municipal (domestic) and industrial sectors for urban areas. If we were to replicate this experiment, then similar results would be anticipated; this is evidenced by the figures in Appendix D2–D6, where many grid cells experiencing unmet demand for irrigation do not experience such a water scarcity for the other sectors. This further supports the development of more flexible prioritization schemes to study related uncertainty in unmet sectoral demands.

While more model development may be needed to represent relevant processes related to human–water interactions, another important aspect to consider is the model evaluation and calibration for hydrological variables. The variables which are the most important for water availability modelling are precipitation, evapotranspiration, snowpack dynamics, glacial melt, soil moisture, surface runoff, river flow, and groundwater levels and recharge. For example, Vanderkelen et al. (2022) showed that while globally the runoff biases in CLM5 are very small ($+0.077\,\mathrm{mm\,d^{-1}}$), large regional biases exist. When aggregated at the level of a catchment, such biases can result in significant river discharge biases, thus limiting the model's usability for water management purposes (Mizukami et al., 2021). Efforts are being made to solve this problem with targeted evaluation studies to better understand the hydrological parameter uncertainty in CLM5 (Yan et al., 2023). At the same time, more efficient and transparent objective calibration protocols to improve model performance for a given set of targets are being developed (Dagon et al., 2020; Cheng et al., 2023). Unfortunately, running large-parameter perturbation ensembles for sensitivity testing and the application of objective calibration protocols remains very expensive for LSMs/ESMs and is usually done only for the release versions of the model. In the future, when the model is calibrated, it could be interesting to expand our analysis by assessing the added value of the implementation of human water management on river flow and other relevant hydrological variables. For example, in the case of GHMs, it was found that considering human-related impacts, including land use change, reservoir operations, and water abstractions, results in a general performance increase to represent streamflow and hydrological extremes (Veldkamp et al., 2018).

Finally, a key limitation of prescribing human water use within ESMs is the potential lack of temporal coherence between atmospheric conditions and sectoral water use. For instance, Huang et al. (2018) used the WATCH Forcing Data methodology applied to ERA-Interim reanalysis data for 1971–2010 (WFDEI; Weedon et al., 2014) for temporal downscaling in the domestic and thermoelectric sectors, using gridded daily air temperature as a proxy. However, a land–atmosphere or fully coupled ESM simulation for the same period, initialized with historically accurate data, may generate atmospheric conditions diverging significantly from observed data due to the model's internal variability (Deser et al., 2012). Currently, there is no known method to fully reconcile these discrepancies.

As an interim measure, one approach is to prescribe sectoral water use data with no monthly temporal variation, effectively distributing it uniformly across the year. The main problem with this approach is that it will greatly limit our ability to understand the impact of hot and dry extremes on water scarcity and sectoral competition. A more suitable solution would be the development of new algorithms for sectoral water use modelling that, similar to irrigation, are prognostic, i.e. dependent on simulated environmental conditions, such as model-computed daily air temperature. In this case, the introduction of our new module offers a useful framework on which such a development can be built.

5 Conclusions

The increasing global challenges surrounding water scarcity highlight the need for advanced modelling tools that can accurately capture human–water interactions. This study makes a contribution in this direction by implementing a data-driven sectoral abstraction module within the Community Earth System Model (CESM) framework. The enhanced model accounts for water abstractions in domestic, livestock, thermoelectric, manufacturing, mining, and irrigation sectors. It closes the water balance by integrating water abstractions from the land component with the supply and return flows from the river component. A basic sectoral competition algorithm was implemented to account for demand–supply dynamics when water availability is below the total demand. As a consequence, water scarcity dynamically emerges in our model and is calculated daily as the gap between local demand and supply for each sector.

We validated the robustness of the implementation of the new sectoral abstraction module in CESM and conducted simulations for the period from 1971 to 2010. These simulations compared a scenario without sectoral water use to one with water use across all sectors. The results were used to analyse the simulated historical global water withdrawal

trends, regional variations in water use, the influence of sectoral water consumption on local climate, and the model's ability to identify known water scarcity hotspots.

While irrigation is the largest user of water globally, we showed that in many regions, other sectors, like domestic or industrial, dominate. This challenges the usual focus on irrigation in Earth system models and points to the increasing importance of non-agricultural water demands in areas experiencing rapid population growth and socio-economic development. Through the implementation of all major water use sectors, it is now possible to study water scarcity in more detail by analysing sector-specific unmet demands and impacts.

Our findings show that only irrigation has the potential to significantly affect local climates (for scales above 100 km), while the effect of non-irrigative sectors is negligible. This might not be true at higher resolutions, especially if we consider groundwater abstractions and land–atmosphere coupling. For example, the Keune et al. (2018) study reveals that groundwater abstraction can significantly weaken the continental sink for atmospheric moisture by reducing soil moisture and altering surface energy fluxes. This reduction in soil moisture leads to decreased evapotranspiration, which in turn can diminish the local recycling of moisture back into the atmosphere. The diminished recycling can lead to reduced precipitation in some regions, thereby exacerbating local drought conditions. Furthermore, the weakening of the continental moisture sink due to groundwater depletion can have far-reaching implications for weather patterns and regional climate stability. While we find that the climatic impacts of other sectors like domestic and industrial water use are comparatively small, their inclusion in the model remains important for water scarcity assessment capabilities.

The model's simulations adeptly capture global hotspots of water scarcity identified in previous research on the topic (Mancosu et al., 2015; Liu et al., 2017). These results are promising and show the potential of CESM and its land component, the Community Land Model (CLM5), as a tool for future water scarcity assessments. In this regard, with the new sectoral water capability, the CLM5 model is well positioned for research on water use and scarcity, paralleling the capabilities of global hydrological models (GHMs). This feature enables the CLM5 to act as an impact model for the water sector, contributing to initiatives such as the Inter-Sectoral Impact Model Intercomparison Project (ISIMIP; Frieler et al., 2017). Additionally, it paves the way for the incorporation of this sectoral water use data into Earth system model (ESM) simulations in a coupled mode. Although the direct feedbacks on climate from this additional sectoral water use are relatively minor, they play an important role in realistically modelling other ESM variables, such as runoff and river flow.

Appendix A: Modelling framework

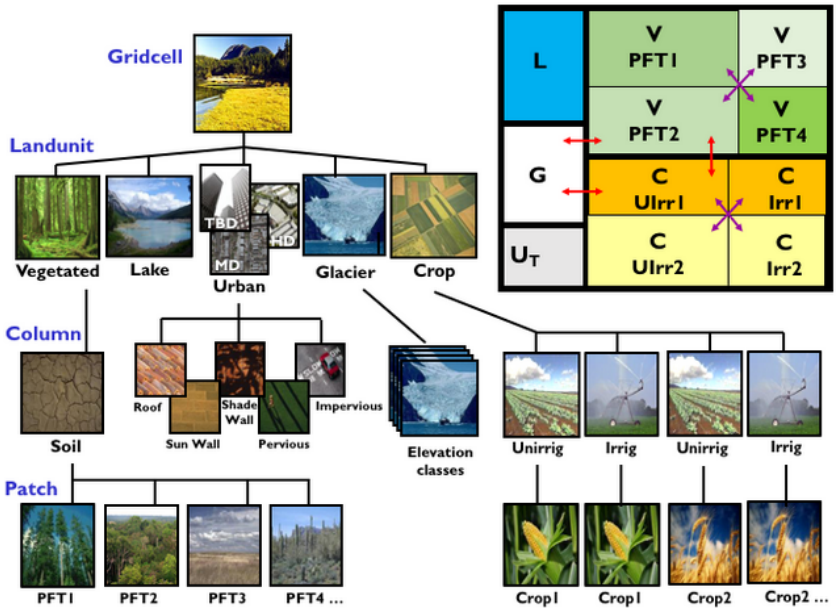

Figure A1. Standard configuration of the CLM5 subgrid hierarchy. The box in the upper right shows the hypothetical subgrid distribution for a single grid cell. Note that the crop land unit is only used when the model is run with the crop model active. TBD is for tall building district; HD is for high density; MD is for medium density; G is for glacier; L is for lake; U is for urban; C is for crop; V is for vegetated; PFT is for plant functional type; Irr is for irrigated; Rnfd is for rainfed. Red arrows indicate allowed land unit transitions. Purple arrows indicate allowed patch level transitions. This figure is taken from Lawrence et al. (2019) and used with the author's permission.

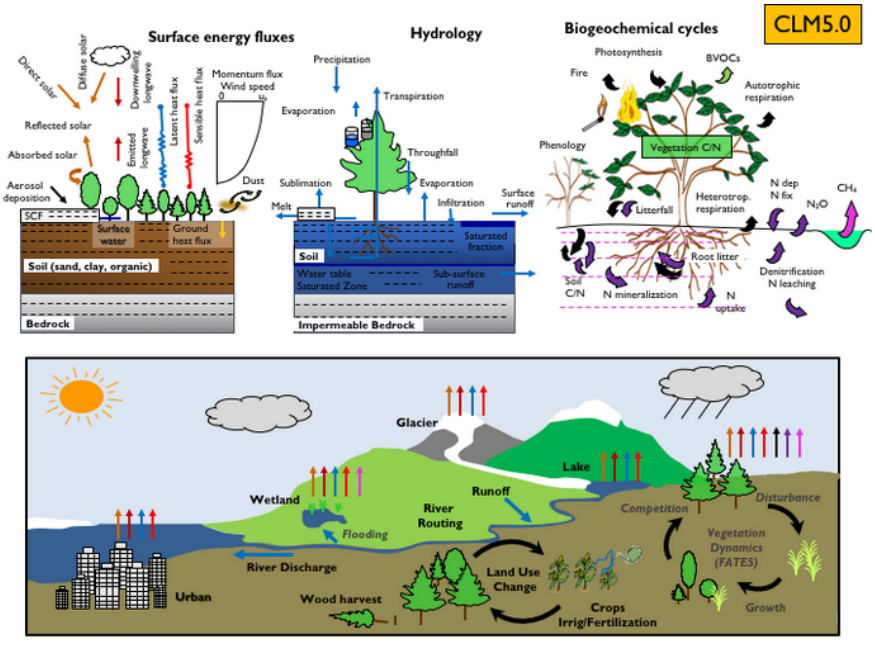

Figure A2. Schematic representation of the primary processes and functionality in CLM5. SCF is for snow cover fraction; BVOC is for biogenic volatile organic compounds; C/N is for carbon and nitrogen. For biogeochemical cycles, the black arrow denotes carbon flux, and the purple arrow denotes nitrogen flux. Note that not all soil levels are shown, and not all processes are depicted. Optional features that are not active in default configurations are italicized. This figure is taken from Lawrence et al. (2019) and used with the author's permission.

Appendix B: Sectoral use module validation

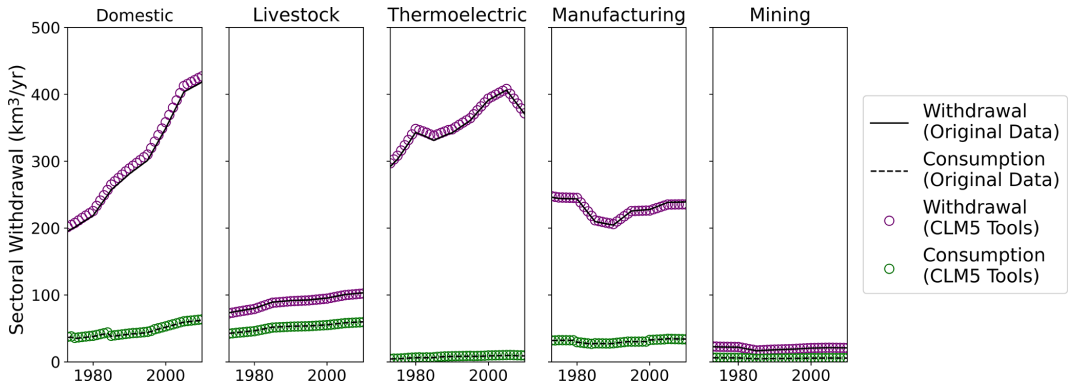

Figure B1. Comparison between global annual sectoral water withdrawal and consumption computed from the original dataset at $0.5 \times 0.5°$ resolution (black lines) and the preprocessed dataset at $0.9 \times 1.25°$ on the CLM5 land mask (coloured circles). The remapping process was done using existing CLM5 tool modules by extending the support for sectoral water use datasets (Taranu, 2024b).

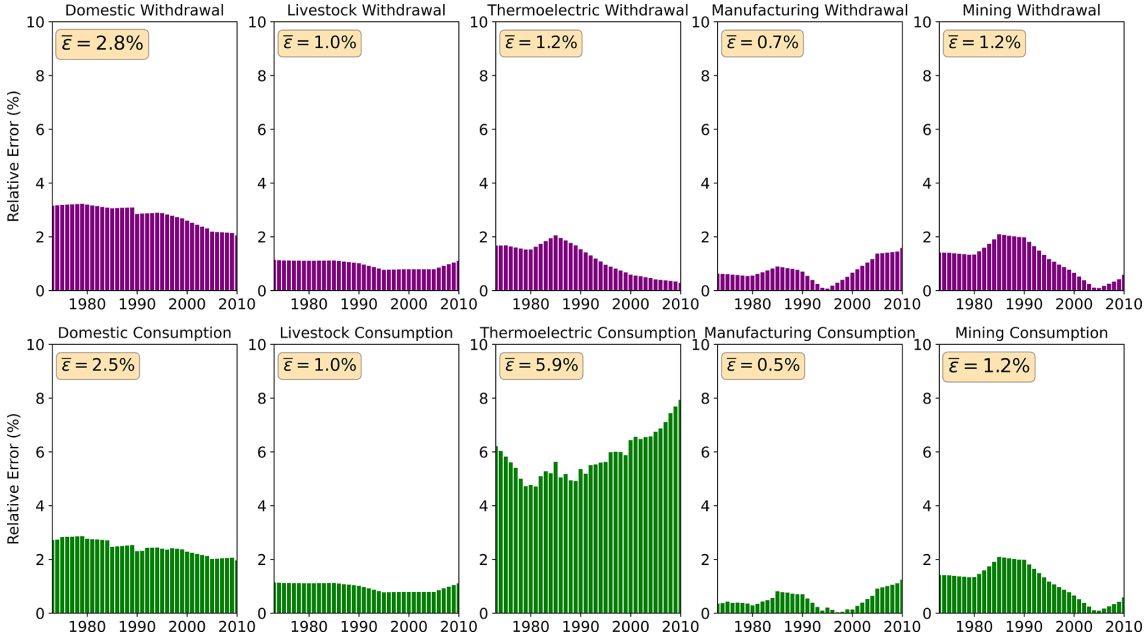

Figure B2. Relative errors between global annual sectoral water withdrawal and consumption computed from the original dataset at $0.5 \times 0.5°$ resolution and the preprocessed dataset $0.9 \times 1.25°$ on the CLM5 land mask (Fig. B1).

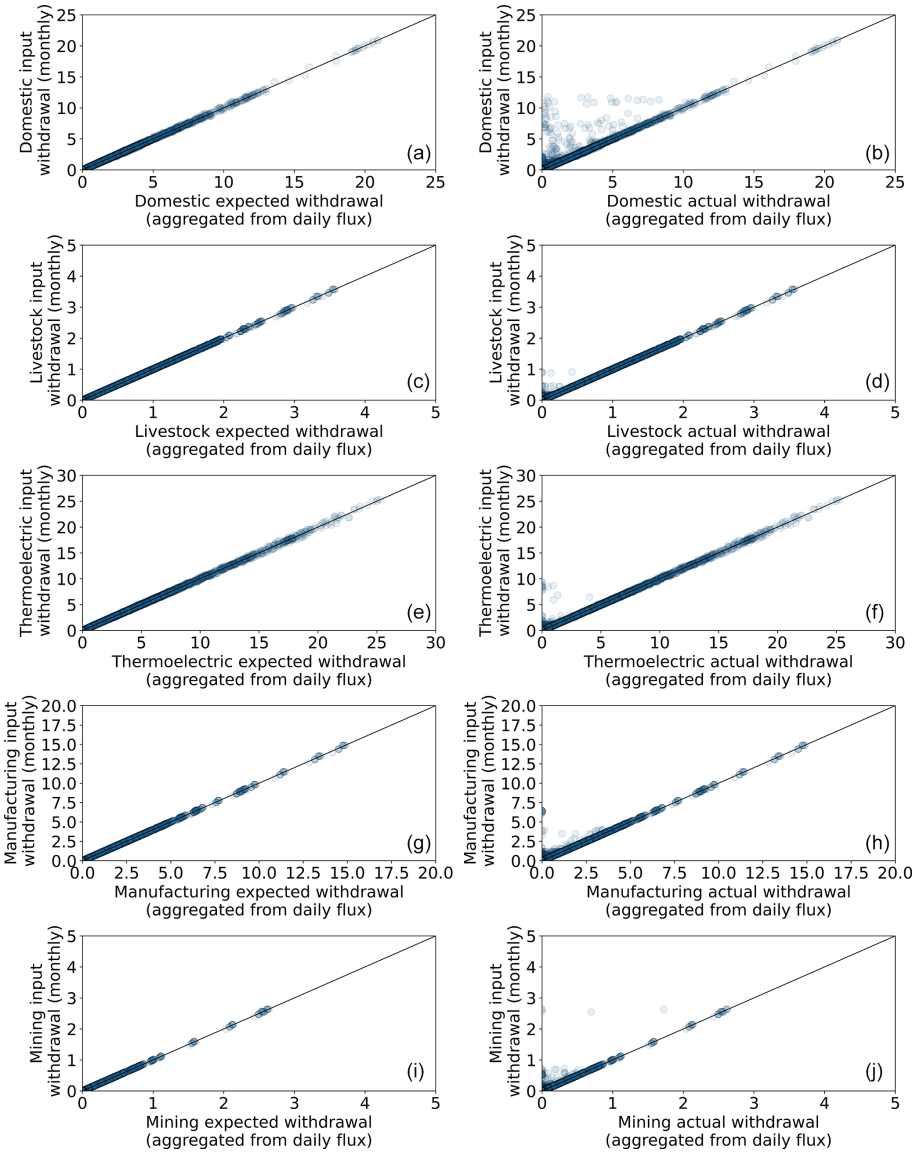

Figure B3. Comparison between expected monthly sectoral withdrawal values from input data and monthly values aggregated from daily expected or actual withdrawal from model outputs. Each point represents the monthly value for a given grid cell. The points are plotted semi-transparently ($\alpha = 0.5$); therefore, the more intense coloured parts simply indicate a larger concentration of the values in that range. This plot was made using the outputs for the year 2000 of the SectorWater experiment, and units for both axes are in millimetres per month (mm month^{-1}).

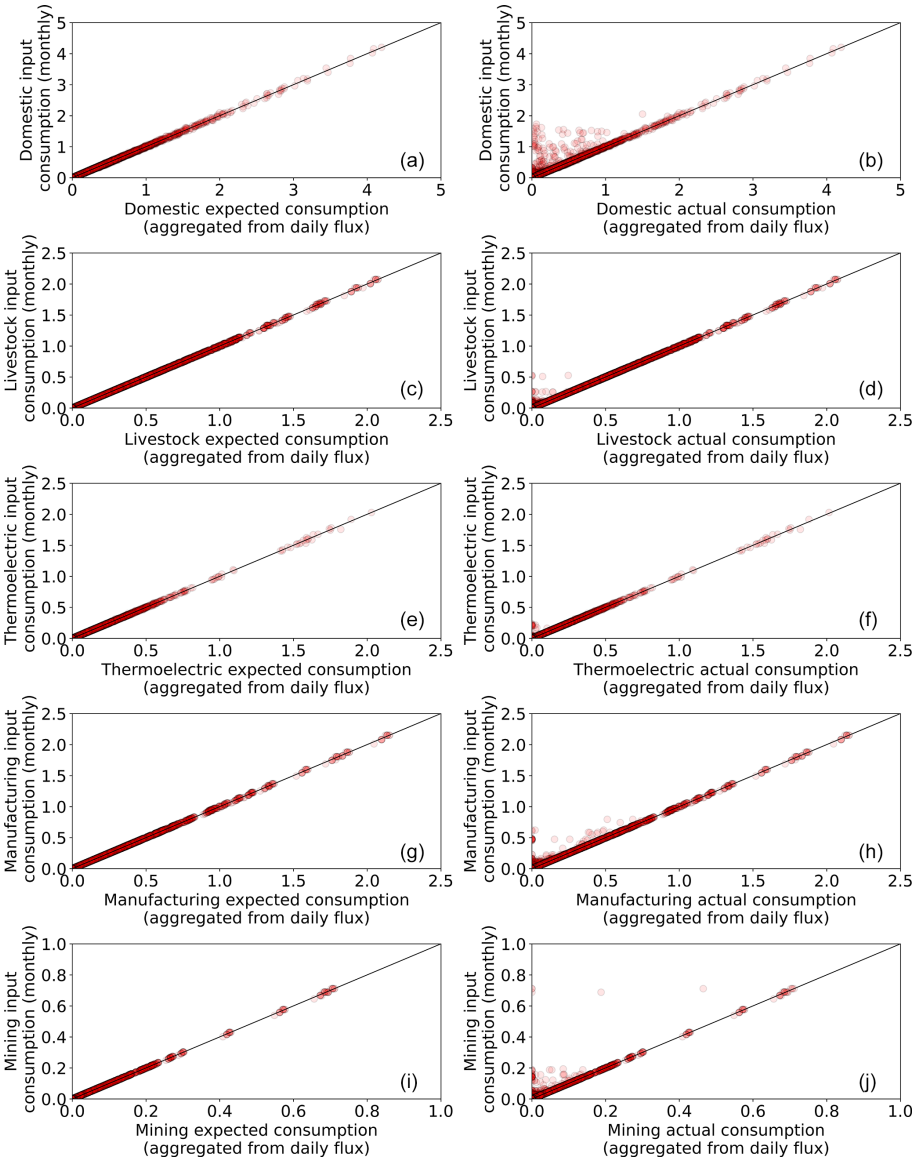

Figure B4. Comparison between expected monthly sectoral consumption values from input data and monthly values aggregated from daily expected or actual consumption from model outputs. Each point represents the monthly value for a given grid cell. The points are plotted semi-transparently ($\alpha = 0.5$); therefore, the more intense coloured parts simply indicate a larger concentration of the values in that range. This plot was made using the outputs for the year 2000 of the SectorWater experiment, and units for both axis are millimetres per month (mm month^{-1}).

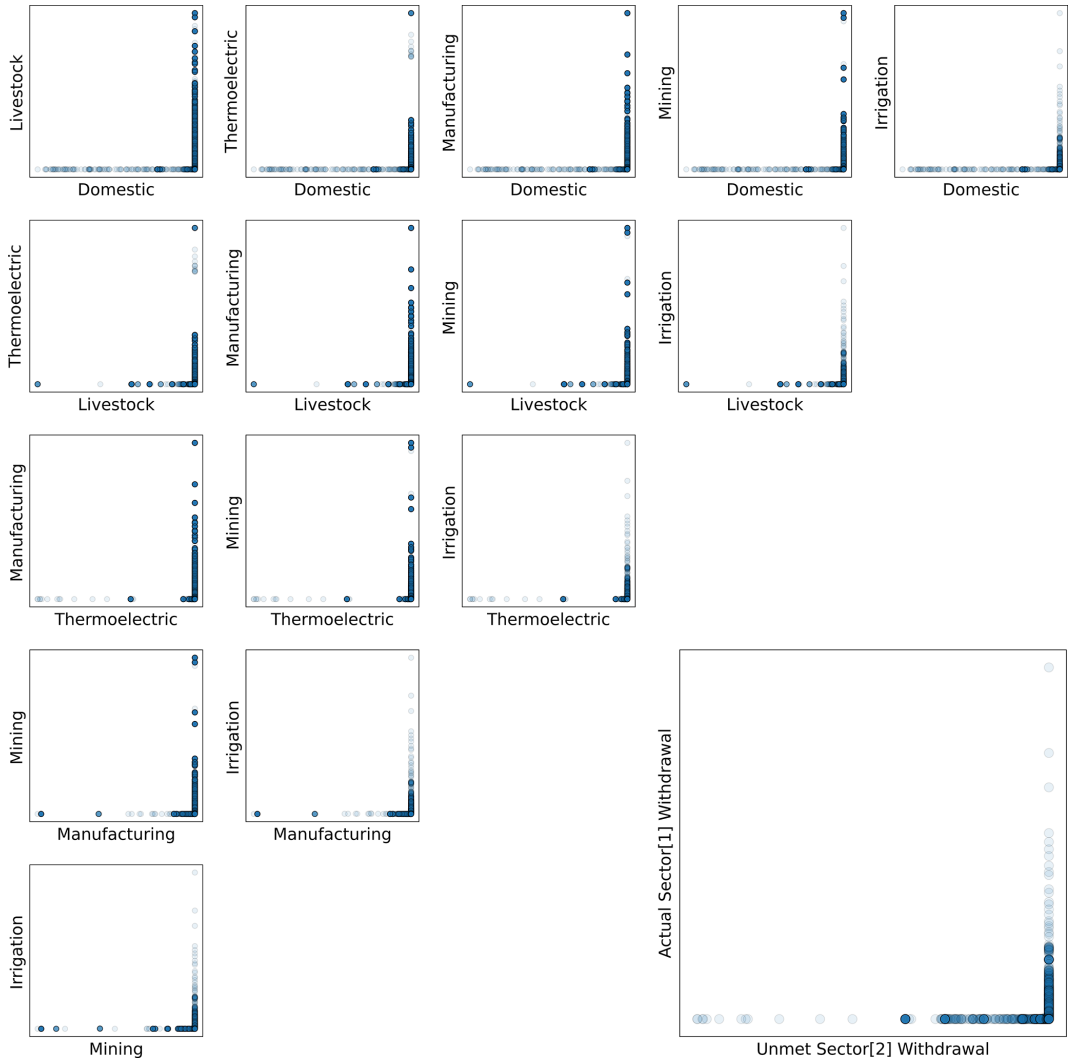

Figure B5. Evaluation of the sectoral competition algorithm, with each point representing a daily value at grid cell level. The points are plotted semi-transparently ($\alpha = 0.5$); therefore, the more intensely coloured parts simply indicate a larger concentration of the values in that range. The plot was made by sampling the first 30 d of the year 2000 from the SectorWater experiment. The intersection between the unsatisfied sectoral withdrawal of the sector higher in priority and the actual withdrawal of the sector lower in priority represents the zero value.

Appendix C: Global trends

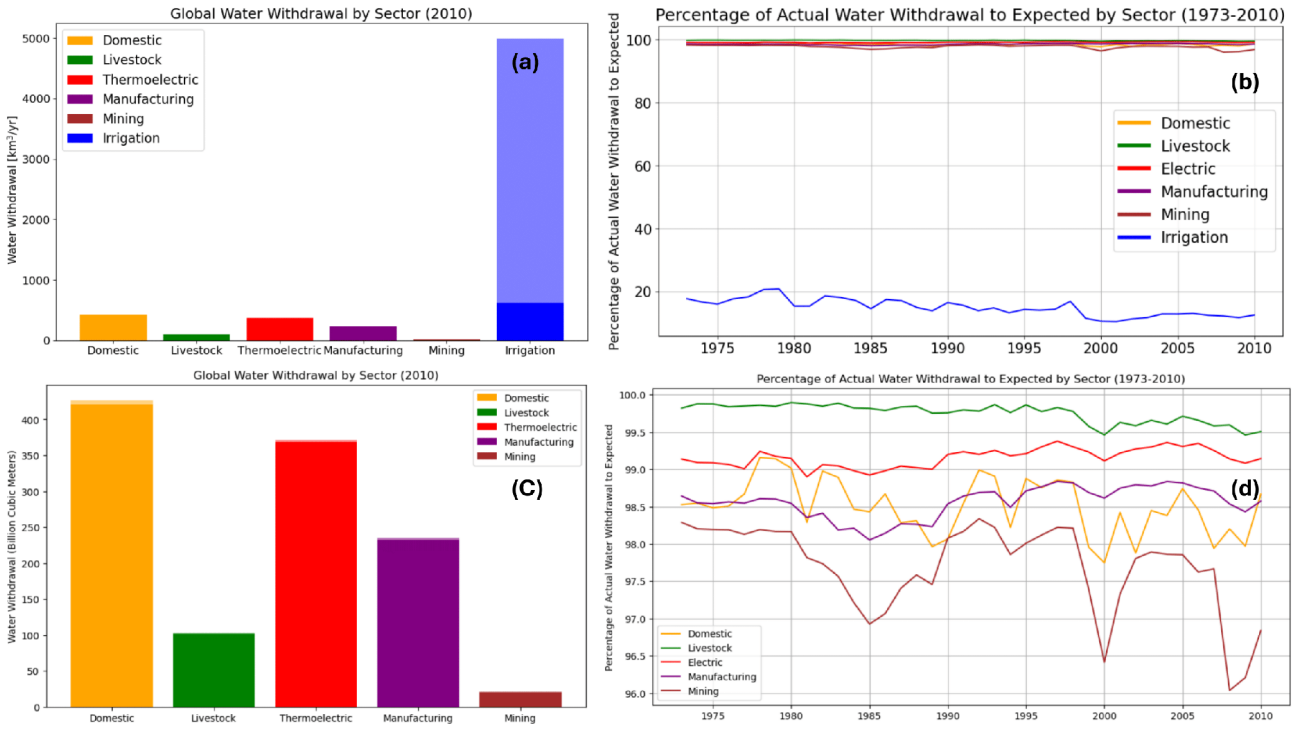

Figure C1. The figure shows the annual global sectoral withdrawal **(a, c)** for the year 2010 and the time series of the global unmet sectoral demand throughout the period 1973–2010 **(b, d)**. Non-irrigative sectors are separate from irrigation in the second row **(c, d)** for better visibility.

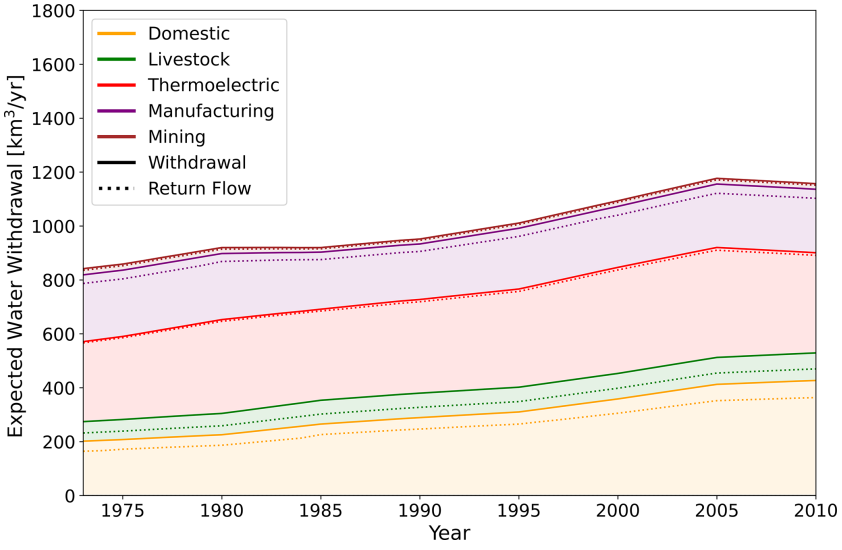

Figure C2. Annual global expected sectoral withdrawal and return flow (without irrigation) throughout the years 1973–2010. This figure was produced using the SectorWater experiment results. It should be noted that the consumption rate in the Huang et al. (2018) dataset for the livestock sector is quite low when compared to other studies (0.4 vs. 1.0). This is explained by the usage of USGS-estimated consumption rates globally, while other models simply assume 100 % consumption.

Appendix D: Streamflow and ocean discharge changes

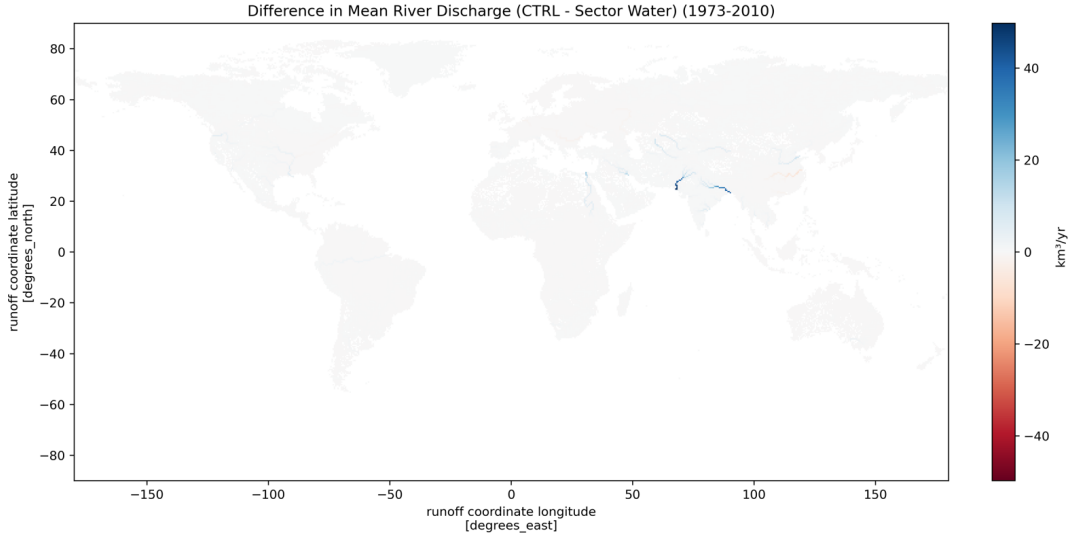

Figure D1. Difference in mean annual river discharge between CTRL and SectorWater experiments.

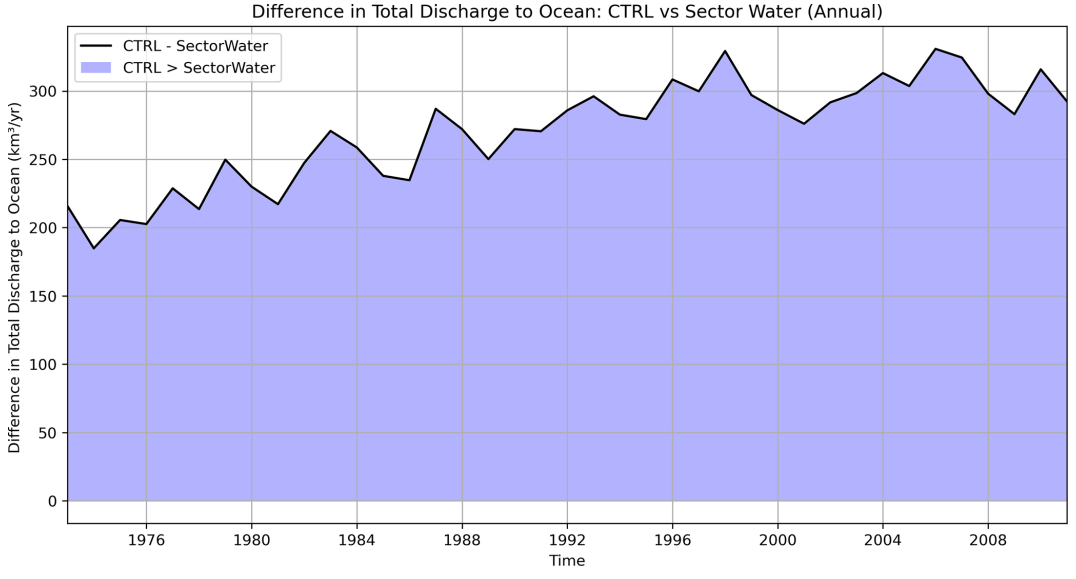

Figure D2. Difference in total annual river discharge to ocean for the period 1973–2010.

Appendix E: Water scarcity

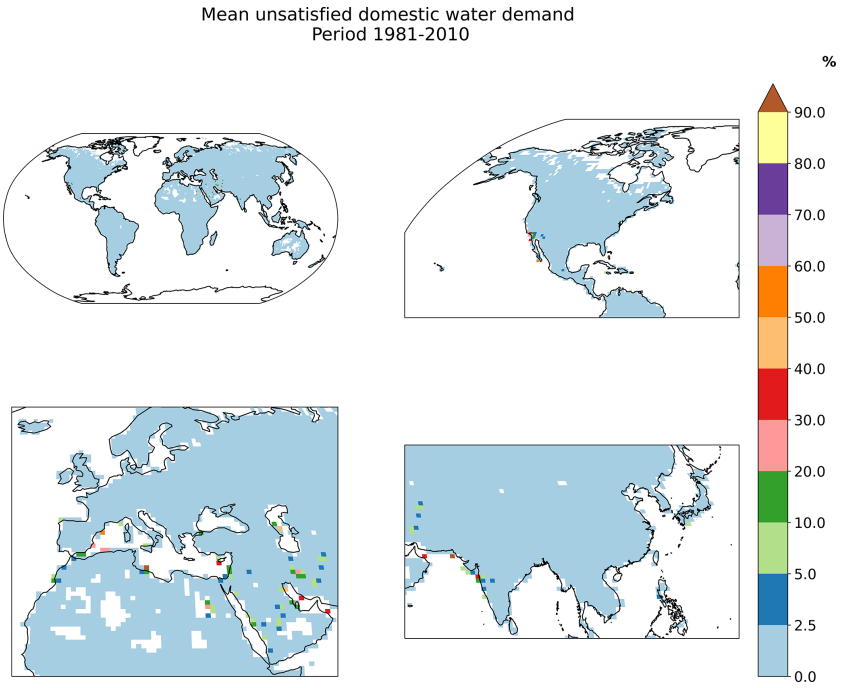

Figure E1. Fraction of unsatisfied domestic demand averaged over a 30-year period (1981–2010). This figure was produced using the SectorWater experiment results by comparing expected vs. actual withdrawal.

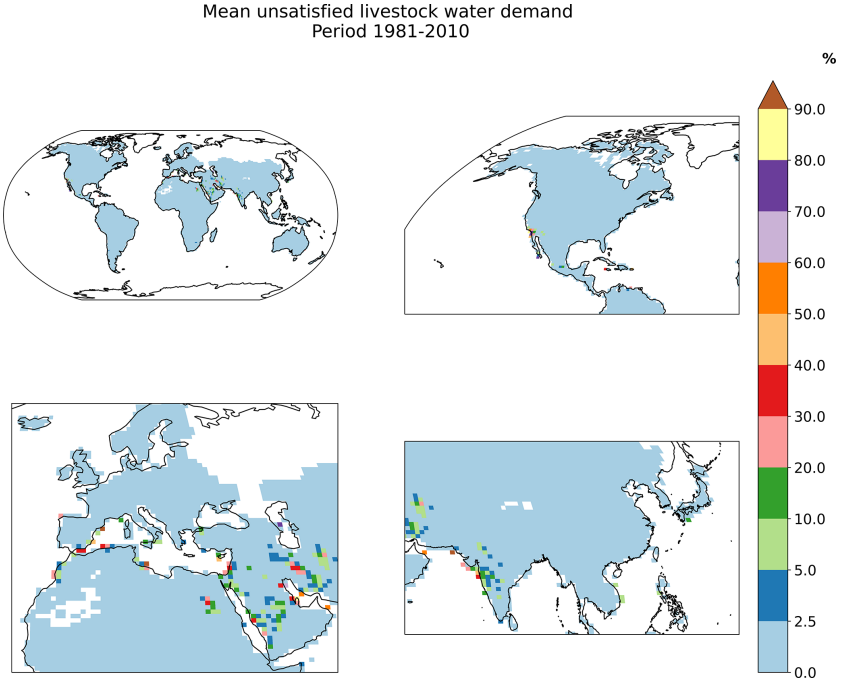

Figure E2. Fraction of unsatisfied livestock demand averaged over a 30-year period (1981–2010). This figure was produced using the SectorWater experiment results by comparing expected vs. actual withdrawal.

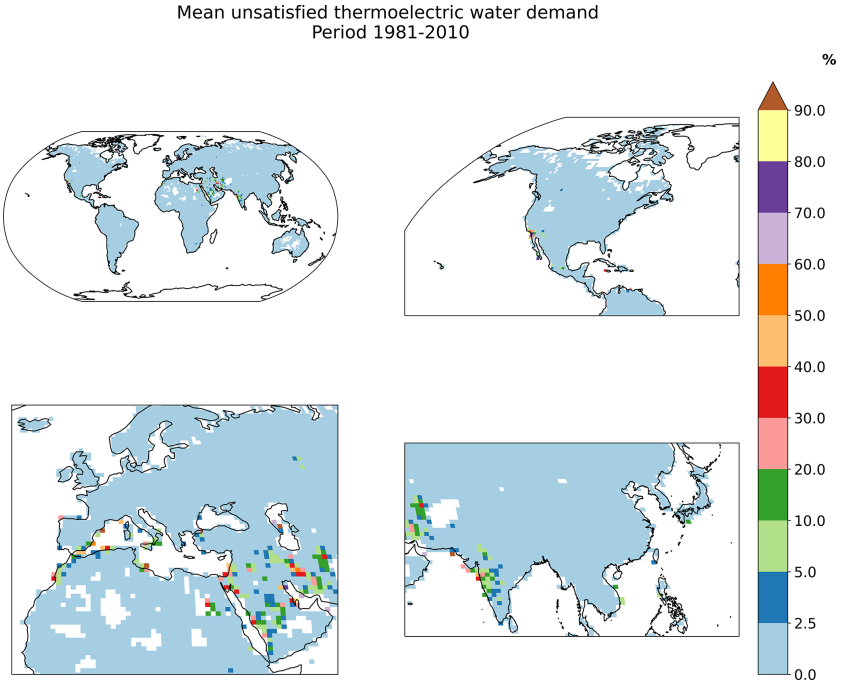

Figure E3. Fraction of unsatisfied thermoelectric demand averaged over a 30-year period (1981–2010). This figure was produced using the SectorWater experiment results by comparing expected vs. actual withdrawal.

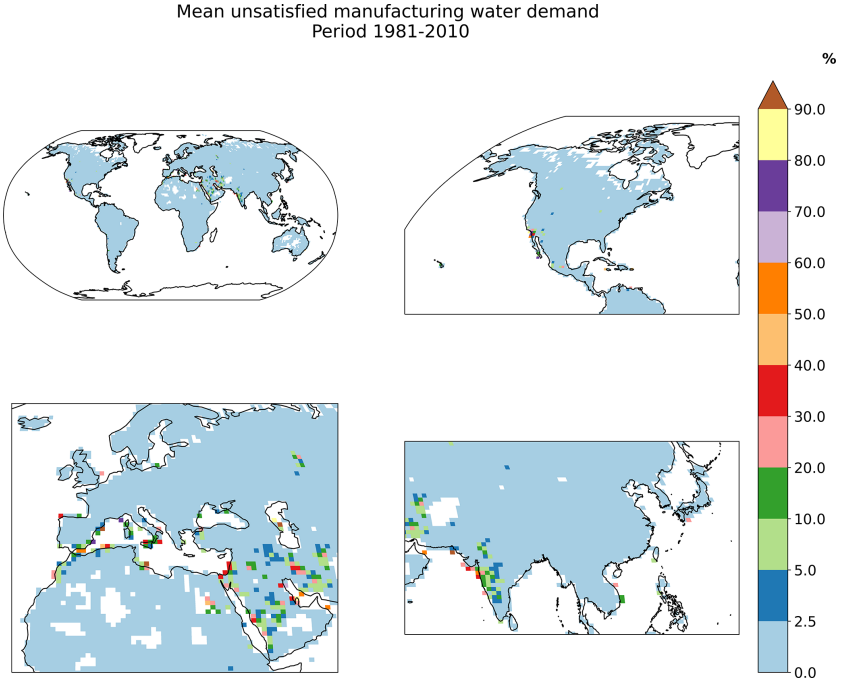

Figure E4. Fraction of unsatisfied manufacturing demand averaged over a 30-year period (1981–2010). This figure was produced using the SectorWater experiment results by comparing expected vs. actual withdrawal.

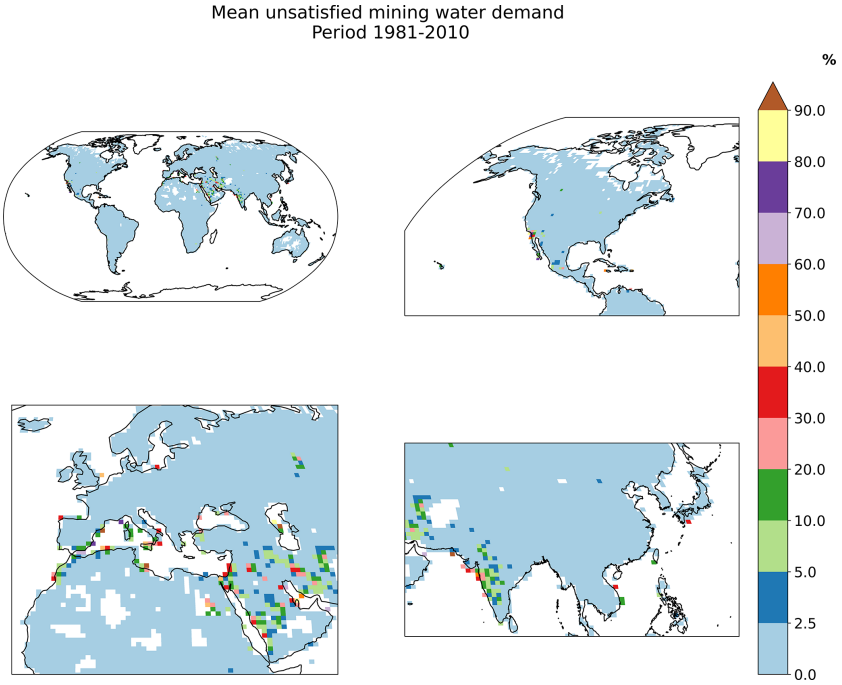

Figure E5. Fraction of unsatisfied mining demand averaged over a 30-year period (1981–2010). This figure was produced using the SectorWater experiment results by comparing expected vs. actual withdrawal.

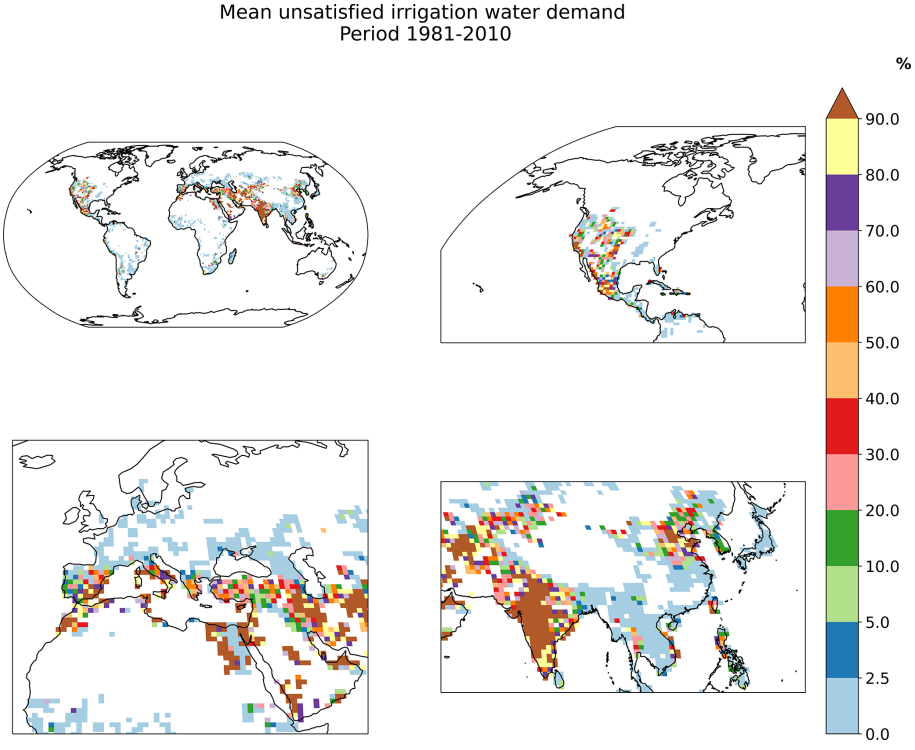

Figure E6. Fraction of unsatisfied irrigation demand averaged over a 30-year period (1981–2010). This figure was produced using the SectorWater experiment results by comparing expected vs. actual withdrawal.

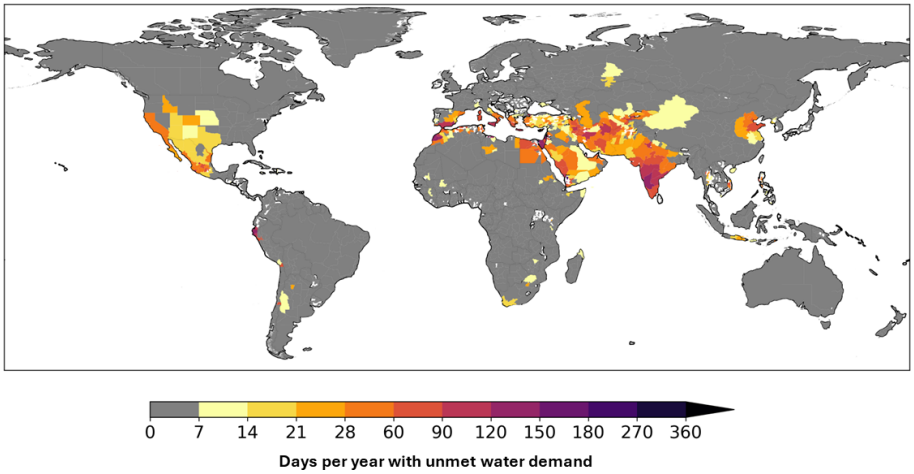

Figure E7. Average number of days per year, from 1973–2010, when modelled water supply was insufficient to meet the demand for all sectors. The values are aggregated at the first administrative division level within each country. Note the non-linear colour bar.

Code and data availability. The model code with the new sectoral water use module, as well as the experiment setups, can be accessed at https://doi.org/10.5281/zenodo.10579224 (Taranu, 2024b). The data needed to reproduce this study can be accessed at https://doi.org/10.5281/zenodo.10518843 (Taranu, 2024c). The scripts used in this study are available at https://github.com/VUB-HYDR/2024_Taranu_etal_GMD (last access: 29 January 2024) and at https://doi.org/10.5281/zenodo.12675434 (Taranu, 2024a).

Author contributions. SIT developed and implemented the new module, made the analysis and visualizations, and wrote the paper. EK, YY, SJDH, and IV provided technical support and feedback during the model development stage. SR did the additional testing of the module and was responsible for the integration of the pull request into the main model branch. DML, YW, TT, and WT supervised the work. All authors actively contributed to the project through regular meetings and provided critical feedback. All authors revised the final version of the paper.

Competing interests. At least one of the (co-)authors is a member of the editorial board of *Geoscientific Model Development*. The peer-review process was guided by an independent editor, and the authors also have no other competing interests to declare.

Disclaimer. Publisher's note: Copernicus Publications remains neutral with regard to jurisdictional claims made in the text, published maps, institutional affiliations, or any other geographical representation in this paper. While Copernicus Publications makes every effort to include appropriate place names, the final responsibility lies with the authors.

Acknowledgements. The authors thank the National Center for Atmospheric Research (NCAR), and in particular the Climate and Global Dynamics Laboratory, for hosting Sabin I. Taranu for a 1-month research stay. We would like to acknowledge high-performance computing support from Cheyenne (https://doi.org/10.5065/D6RX99HX, Computational and Information Systems Laboratory, 2019) provided by NCAR's Computational and Information Systems Laboratory and sponsored by the National Science Foundation.

The authors thank the International Institute for Applied Systems Analysis, and in particular the Water Security group, for accommodating Sabin I. Taranu for a 3-month research stay and sharing their experience in developing global hydrological models.

The authors thank Sean Swenson, Naoki Mizukami, Andy Wood, Will Wieder, Ann Van Griensven, and Steven Eisenreich for their critical feedback on the new module implementation, possible limitations, and potential improvements.

ChatGPT (GPT-4; OpenAI's large-scale language-generation model) was used to improve the writing style of this article. Sabin I. Taranu reviewed, edited, and revised the ChatGPT-generated texts to his own liking and ultimately takes responsibility for the content of this publication.

Financial support. This research has been supported by the European Union's Horizon 2021 research and innovation programme under the Marie Skłodowska-Curie Actions European Training Network, MSCA-ITN-ETN (grant no. 956623), and the inventWater (Inventive forecasting tools for adapting water quality management to a new climate) Project.

Review statement. This paper was edited by Le Yu and reviewed by Wen-Ying Wu and two anonymous referees.

References

Anderson, R. G., Lo, M.-H., Swenson, S., Famiglietti, J. S., Tang, Q., Skaggs, T. H., Lin, Y.-H., and Wu, R.-J.: Using satellite-based estimates of evapotranspiration and groundwater changes to determine anthropogenic water fluxes in land surface models, Geosci. Model Dev., 8, 3021–3031, https://doi.org/10.5194/gmd-8-3021-2015, 2015.

Arias, P. A., Bellouin, N., Coppola, E., Jones, R. G., Krinner, G., Marotzke, J., Naik, V., Palmer, M. D., Plattner, G.-K., Rogelj, J., Rojas, M., Sillmann, J., Storelvmo, T., Thorne, P. W., Trewin, B., Achuta Rao, K., Adhikary, B., Allan, R. P., Armour, K., Bala, G., Barimalala, R., Berger, S., Canadell, J. G., Cassou, C., Cherchi, A., Collins, W., Collins, W. D., Connors, S. L., Corti, S., Cruz, F., Dentener, F. J., Dereczynski, C., Di Luca, A., Diongue Niang, A., Doblas-Reyes, F. J., Dosio, A., Douville, H., Engelbrecht, F., Eyring, V., Fischer, E., Forster, P., Fox-Kemper, B., Fuglestvedt, J. S., Fyfe, J. C., Gillett, N. P., Goldfarb, L., Gorodetskaya, I., Gutierrez, J. M., Hamdi, R., Hawkins, E., Hewitt, H. T., Hope, P., Islam, A. S., Jones, C., Kaufman, D. S., Kopp, R. E., Kosaka, Y., Kossin, J., Krakovska, S., Lee, J.-Y., Li, J., Mauritsen, T., Maycock, T. K., Meinshausen, M., Min, S.-K., Monteiro, P. M. S., Ngo-Duc, T., Otto, F., Pinto, I., Pirani, A., Raghavan, K., Ranasinghe, R., Ruane, A. C., Ruiz, L., Sallée, J.-B., Samset, B. H., Sathyendranath, S., Seneviratne, S. I., Sörensson, A. A., Szopa, S., Takayabu, I., Tréguier, A.-M., van den Hurk, B., Vautard, R., von Schuckmann, K., Zaehle, S., Zhang, X., and Zickfeld, K.: Technical Summary, in: Climate Change 2021: The Physical Science Basis, Contribution of Working Group I to the Sixth Assessment Report of the Intergovernmental Panel on Climate Change, edited by: Masson-Delmotte, V., Zhai, P., Pirani, A., Connors, S. L., Péan, C., Berger, S., Caud, N., Chen, Y., Goldfarb, L., Gomis, M. I., Huang, M., Leitzell, K., Lonnoy, E., Matthews, J. B. R., Maycock, T. K., Waterfield, T., Yelekçi, O., Yu, R., and Zhou, B., Cambridge University Press, Cambridge, United Kingdom and New York, NY, USA, 33−-144, https://doi.org/10.1017/9781009157896.002, 2021.

Arnell, N. W. and Lloyd-Hughes, B.: The global-scale impacts of climate change on water resources and flooding under new climate and socio-economic scenarios, Clim. Change, 122, 127–140, https://doi.org/10.1007/s10584-013-0948-4, 2014.

Baccini, A., Walker, W., Carvalho, L., Farina, M., Sulla-Menashe, D., and Houghton, R. A.: Tropical forests are a net carbon source based on aboveground measurements of gain and loss, Science, 13, 230–234, https://doi.org/10.1126/science.aam5962, 2017.

Bakker, K.: Water Security: Research Challenges and Opportunities, Science, 337, 914–915, https://doi.org/10.1126/science.1226337, 2012.

Becken, S.: Water equity – Contrasting tourism water use with that of the local community, Water Resources and Industry, 7–8, 9–22, https://doi.org/10.1016/j.wri.2014.09.002, 2014.

Best, J.: Anthropogenic stresses on the world's big rivers, Nat. Geosci., 12, 7–21, https://doi.org/10.1038/s41561-018-0262-x, 2019.

Bierkens, M. F. P. and Wada, Y.: Non-renewable groundwater use and groundwater depletion: a review, Environ. Res. Lett., 14, 063002, https://doi.org/10.1088/1748-9326/ab1a5f, 2019.

Blyth, E. M., Arora, V. K., Clark, D. B., Dadson, S. J., De Kauwe, M. G., Lawrence, D. M., Melton, J. R., Pongratz, J., Turton, R. H., Yoshimura, K., and Yuan, H.: Advances in Land Surface Modelling, Curr. Clim. Change Rep., 7, 45–71, https://doi.org/10.1007/s40641-021-00171-5, 2021.

Burek, P., Satoh, Y., Kahil, T., Tang, T., Greve, P., Smilovic, M., Guillaumot, L., Zhao, F., and Wada, Y.: Development of the Community Water Model (CWatM v1.04) – a high-resolution hydrological model for global and regional assessment of integrated water resources management, Geosci. Model Dev., 13, 3267–3298, https://doi.org/10.5194/gmd-13-3267-2020, 2020.

Cai, Y., Wang, H., Yue, W., Xie, Y., and Liang, Q.: An integrated approach for reducing spatially coupled water-shortage risks of Beijing-Tianjin-Hebei urban agglomeration in China, J. Hydrol., 603, 127123, https://doi.org/10.1016/j.jhydrol.2021.127123, 2021.

Cárdenas Belleza, G. A., Bierkens, M. F. P., and Van Vliet, M. T. H.: Sectoral water use responses to droughts and heatwaves: analyses from local to global scales for 1990–2019, Environ. Res. Lett., 18, 104008, https://doi.org/10.1088/1748-9326/acf82e, 2023.

Chen, L. and Dirmeyer, P. A.: Global observed and modelled impacts of irrigation on surface temperature, Int. J. Climatol., 39, 2587–2600, https://doi.org/10.1002/joc.5973, 2019.

Cheng, Y., Musselman, K. N., Swenson, S., Lawrence, D., Hamman, J., Dagon, K., Kennedy, D., and Newman, A. J.: Moving Land Models Toward More Actionable Science: A Novel Application of the Community Terrestrial Systems Model Across Alaska and the Yukon River Basin, Water Resour. Res., 59, e2022WR032204, https://doi.org/10.1029/2022WR032204, 2023.

Coe, M. T., Costa, M. H., and Soares-Filho, B. S.: The influence of historical and potential future deforestation on the stream flow of the Amazon River – Land surface processes and atmospheric feedbacks, J. Hydrol., 369, 165–174, https://doi.org/10.1016/j.jhydrol.2009.02.043, 2009.

Computational and Information Systems Laboratory: Cheyenne: HPE/SGI ICE XA System (U.S. NSF NCAR Community Computing), Boulder, CO, U.S. National Science Foundation National Center for Atmospheric Research, https://doi.org/10.5065/D6RX99HX, 2019.

Curto, D., Franzitta, V., and Guercio, A.: A Review of the Water Desalination Technologies, Appl. Sci., 11, 670, https://doi.org/10.3390/app11020670, 2021.

Dagon, K., Sanderson, B. M., Fisher, R. A., and Lawrence, D. M.: A machine learning approach to emulation and biophysical parameter estimation with the Community Land Model, version 5, Adv. Stat. Clim. Meteorol. Oceanogr., 6, 223–244, https://doi.org/10.5194/ascmo-6-223-2020, 2020.

Danabasoglu, G., Lamarque, J.-F., Bacmeister, J., Bailey, D. A., DuVivier, A. K., Edwards, J., Emmons, L. K., Fasullo, J., Garcia, R., Gettelman, A., Hannay, C., Holland, M. M., Large, W. G., Lauritzen, P. H., Lawrence, D. M., Lenaerts, J. T. M., Lindsay, K., Lipscomb, W. H., Mills, M. J., Neale, R., Oleson, K. W., Otto-Bliesner, B., Phillips, A. S., Sacks, W., Tilmes, S., Kampenhout, L., Vertenstein, M., Bertini, A., Dennis, J., Deser, C., Fischer, C., Fox-Kemper, B., Kay, J. E., Kinnison, D., Kushner, P. J., Larson, V. E., Long, M. C., Mickelson, S., Moore, J. K., Nienhouse, E., Polvani, L., Rasch, P. J., and Strand, W. G.: The Community Earth System Model Version 2 (CESM2), J. Adv. Model. Earth Sy., 12, e2019MS001916, https://doi.org/10.1029/2019MS001916, 2020.

Davidson, N. C.: How much wetland has the world lost? Long-term and recent trends in global wetland area, Mar. Freshwater Res., 65, 934–941, https://doi.org/10.1071/MF14173, 2014.

de Graaf, I. E. M., Gleeson, T., Rens van Beek, L. P. H., Sutanudjaja, E. H. and Bierkens, M. F. P.: Environmental flow limits to global groundwater pumping, Nature, 574, 90–94, https://doi.org/10.1038/s41586-019-1594-4, 2019.

De Hertog, S. J., Havermann, F., Vanderkelen, I., Guo, S., Luo, F., Manola, I., Coumou, D., Davin, E. L., Duveiller, G., Lejeune, Q., Pongratz, J., Schleussner, C.-F., Seneviratne, S. I., and Thiery, W.: The biogeophysical effects of idealized land cover and land management changes in Earth system models, Earth Syst. Dynam., 14, 629–667, https://doi.org/10.5194/esd-14-629-2023, 2023.

Deser, C., Phillips, A., Bourdette, V., and Teng, H.: Uncertainty in climate change projections: the role of internal variability, Clim. Dynam., 38, 527–546, https://doi.org/10.1007/s00382-010-0977-x, 2012.

Dolan, F., Lamontagne, J., Link, R., Hejazi, M., Reed, P., and Edmonds, J.: Evaluating the economic impact of water scarcity in a changing world, Nat. Commun., 12, 1915, https://doi.org/10.1038/s41467-021-22194-0, 2021.

Döll, P. and Schmied, H. M.: How is the impact of climate change on river flow regimes related to the impact on mean annual runoff? A global-scale analysis, Environ. Res. Lett., 7, 014037, https://doi.org/10.1088/1748-9326/7/1/014037, 2012.

Döll, P., Hoffmann-Dobrev, H., Portmann, F. T., Siebert, S., Eicker, A., Rodell, M., Strassberg, G., and Scanlon, B. R.: Impact of water withdrawals from groundwater and surface water on continental water storage variations, J. Geodynam., 59–60, 143–156, https://doi.org/10.1016/j.jog.2011.05.001, 2012.

Drijfhout, S., Bathiany, S., Beaulieu, C., Brovkin, V., Claussen, M., Huntingford, C., Scheffer, M., Sgubin, G., and Swingedouw, D.: Catalogue of abrupt shifts in Intergovernmental Panel on Climate Change climate models, P. Natl. Acad. Sci. USA, 112, E5777–E5786, https://doi.org/10.1073/pnas.1511451112, 2015.

Droppers, B., Franssen, W. H. P., van Vliet, M. T. H., Nijssen, B., and Ludwig, F.: Simulating human impacts on global water resources using VIC-5, Geosci. Model Dev., 13, 5029–5052, https://doi.org/10.5194/gmd-13-5029-2020, 2020.

Eke, J., Yusuf, A., Giwa, A., and Sodiq, A.: The global status of desalination: An assessment of current desalination technologies, plants and capacity, Desalination, 495, 114633, https://doi.org/10.1016/j.desal.2020.114633, 2020.

Eyring, V., Bony, S., Meehl, G. A., Senior, C. A., Stevens, B., Stouffer, R. J., and Taylor, K. E.: Overview of the Coupled Model Intercomparison Project Phase 6 (CMIP6) experimental design and organization, Geosci. Model Dev., 9, 1937–1958, https://doi.org/10.5194/gmd-9-1937-2016, 2016.

Famiglietti, J: The global groundwater crisis, Nat. Clim. Change 4, 945–948, https://doi.org/10.1038/nclimate2425, 2014.

Felfelani, F., Lawrence, D. M., and Pokhrel, Y.: Representing Intercell Lateral Groundwater Flow and Aquifer Pumping in the Community Land Model, Water Resour. Res., 57, e2020WR027531, https://doi.org/10.1029/2020WR027531, 2021.

Flörke, M., Kynast, E., Bärlund, I., Eisner, S., Wimmer, F., and Alcamo, J.: Domestic and industrial water uses of the past 60 years as a mirror of socio-economic development: A global simulation study, Global Environ. Change, 23, 144–156, https://doi.org/10.1016/j.gloenvcha.2012.10.018, 2013.

Foley, J. A., DeFries, R., Asner, G. P., Barford, C., Bonan, G., Carpenter, S. R., Chapin, F. S., Coe, M. T., Daily, G. C., Gibbs, H. K., Helkowski, J. H., Holloway, T., Howard, E. A., Kucharik, C. J., Monfreda, C., Patz, J. A., Prentice, I. C., Ramankutty, N., and Snyder, P. K.: Global Consequences of Land Use, Science 309, 570–574, https://doi.org/10.1126/science.1111772, 2005.

Frieler, K., Lange, S., Piontek, F., Reyer, C. P. O., Schewe, J., Warszawski, L., Zhao, F., Chini, L., Denvil, S., Emanuel, K., Geiger, T., Halladay, K., Hurtt, G., Mengel, M., Murakami, D., Ostberg, S., Popp, A., Riva, R., Stevanovic, M., Suzuki, T., Volkholz, J., Burke, E., Ciais, P., Ebi, K., Eddy, T. D., Elliott, J., Galbraith, E., Gosling, S. N., Hattermann, F., Hickler, T., Hinkel, J., Hof, C., Huber, V., Jägermeyr, J., Krysanova, V., Marcé, R., Müller Schmied, H., Mouratiadou, I., Pierson, D., Tittensor, D. P., Vautard, R., van Vliet, M., Biber, M. F., Betts, R. A., Bodirsky, B. L., Deryng, D., Frolking, S., Jones, C. D., Lotze, H. K., Lotze-Campen, H., Sahajpal, R., Thonicke, K., Tian, H., and Yamagata, Y.: Assessing the impacts of 1.5 °C global warming – simulation protocol of the Inter-Sectoral Impact Model Intercomparison Project (ISIMIP2b), Geosci. Model Dev., 10, 4321–4345, https://doi.org/10.5194/gmd-10-4321-2017, 2017.

Grill, G., Lehner, B., Lumsdon, A. E., MacDonald, G. K., Zarfl, C., and Reidy Liermann, C.: An index-based framework for assessing patterns and trends in river fragmentation and flow regulation by global dams at multiple scales, Environ. Res. Lett., 10, 015001, https://doi.org/10.1088/1748-9326/10/1/015001, 2015.

Hanasaki, N., Kanae, S., and Oki, T.: A reservoir operation scheme for global river routing models, J. Hydrol., 327, 22–41, https://doi.org/10.1016/j.jhydrol.2005.11.011, 2006.

Hanasaki, N., Yoshikawa, S., Kakinuma, K., and Kanae, S.: A seawater desalination scheme for global hydrological models, Hydrol. Earth Syst. Sci., 20, 4143–4157, https://doi.org/10.5194/hess-20-4143-2016, 2016.

Hanasaki, N., Yoshikawa, S., Pokhrel, Y., and Kanae, S.: A global hydrological simulation to specify the sources of water used by humans, Hydrol. Earth Syst. Sci., 22, 789–817, https://doi.org/10.5194/hess-22-789-2018, 2018.

Hejazi, M. I., Edmonds, J., Clarke, L., Kyle, P., Davies, E., Chaturvedi, V., Wise, M., Patel, P., Eom, J., and Calvin, K.: Integrated assessment of global water scarcity over the 21st century under multiple climate change mitigation policies, Hydrol. Earth Syst. Sci., 18, 2859–2883, https://doi.org/10.5194/hess-18-2859-2014, 2014.

Hejazi, M. I., Voisin, N., Liu, L., Bramer, L. M., Fortin, D. C., Hathaway, J. E., Huang, M., Kyle, P., Leung, L. R., Li, H.-Y., Liu, Y., Patel, P. L., Pulsipher, T. C., Rice, J. S., Tesfa, T. K., Vernon, C. R., and Zhou, Y.: 21st century United States emissions mitigation could increase water stress more than the climate change it is mitigating, P. Natl. Acad. Sci. USA, 112, 10635–10640, https://doi.org/10.1073/pnas.1421675112, 2015.

Hoekstra, A. Y., Mekonnen, M. M., Chapagain, A. K., Mathews, R. E., and Richter, B. D.: Global Monthly Water Scarcity: Blue Water Footprints versus Blue Water Availability, PLoS ONE 7, e32688, https://doi.org/10.1371/journal.pone.0032688, 2012.

Huang, Z., Hejazi, M., Li, X., Tang, Q., Vernon, C., Leng, G., Liu, Y., Döll, P., Eisner, S., Gerten, D., Hanasaki, N., and Wada, Y.: Reconstruction of global gridded monthly sectoral

water withdrawals for 1971–2010 and analysis of their spatiotemporal patterns, Hydrol. Earth Syst. Sci., 22, 2117–2133, https://doi.org/10.5194/hess-22-2117-2018, 2018.

Jägermeyr, J., Gerten, D., Heinke, J., Schaphoff, S., Kummu, M., and Lucht, W.: Water savings potentials of irrigation systems: global simulation of processes and linkages, Hydrol. Earth Syst. Sci., 19, 3073–3091, https://doi.org/10.5194/hess-19-3073-2015, 2015.

Jevrejeva, S., Jackson, L. P., Riva, R. E. M., Grinsted, A., and Moore, J. C.: Coastal sea level rise with warming above 2 °C, P. Natl. Acad. Sci. USA, 113, 13342–13347, https://doi.org/10.1073/pnas.1605312113, 2016.

Jones, E., Qadir, M., Van Vliet, M. T. H., Smakhtin, V., and Kang, S.: The state of desalination and brine production: A global outlook, Sci. Total Environ., 657, 1343–1356, https://doi.org/10.1016/j.scitotenv.2018.12.076, 2019.

Jones, E. R., van Vliet, M. T. H., Qadir, M., and Bierkens, M. F. P.: Country-level and gridded estimates of wastewater production, collection, treatment and reuse, Earth Syst. Sci. Data, 13, 237–254, https://doi.org/10.5194/essd-13-237-2021, 2021.

Jones, E. R., Bierkens, M. F. P., Wanders, N., Sutanudjaja, E. H., van Beek, L. P. H., and van Vliet, M. T. H.: DynQual v1.0: a high-resolution global surface water quality model, Geosci. Model Dev., 16, 4481–4500, https://doi.org/10.5194/gmd-16-4481-2023, 2023.

Keune, J., Sulis, M., Kollet, S., Siebert, S., and Wada, Y.: Human water use impacts on the strength of the continental sink for atmospheric water, Geophys. Res. Lett., 45, 4068–4076, https://doi.org/10.1029/2018GL077621, 2018.

Khan, Z., Thompson, I., Vernon, C. R., Graham, N. T., Wild, T. B., and Chen, M.: Global monthly sectoral water use for 2010–2100 at 0.5° resolution across alternative futures, Sci. Data, 10, 201, https://doi.org/10.1038/s41597-023-02086-2, 2023.

Kummu, M., Guillaume, J. H. A., De Moel, H., Eisner, S., Flörke, M., Porkka, M., Siebert, S., Veldkamp, T. I. E., and Ward, P. J.: The world's road to water scarcity: shortage and stress in the 20th century and pathways towards sustainability, Sci. Rep.-UK, 6, 38495, https://doi.org/10.1038/srep38495, 2016.

Lawrence, D. M., Hurtt, G. C., Arneth, A., Brovkin, V., Calvin, K. V., Jones, A. D., Jones, C. D., Lawrence, P. J., de Noblet-Ducoudré, N., Pongratz, J., Seneviratne, S. I., and Shevliakova, E.: The Land Use Model Intercomparison Project (LUMIP) contribution to CMIP6: rationale and experimental design, Geosci. Model Dev., 9, 2973–2998, https://doi.org/10.5194/gmd-9-2973-2016, 2016.

Lawrence, D. M., Fisher, R. A., Koven, C. D., Oleson, K. W., Swenson, S. C., Bonan, G., Collier, N., Ghimire, B., Van Kampenhout, L., Kennedy, D., Kluzek, E., Lawrence, P. J., Li, F., Li, H., Lombardozzi, D., Riley, W. J., Sacks, W. J., Shi, M., Vertenstein, M., Wieder, W. R., Xu, C., Ali, A. A., Badger, A. M., Bisht, G., Van Den Broeke, M., Brunke, M. A., Burns, S. P., Buzan, J., Clark, M., Craig, A., Dahlin, K., Drewniak, B., Fisher, J. B., Flanner, M., Fox, A. M., Gentine, P., Hoffman, F., Keppel-Aleks, G., Knox, R., Kumar, S., Lenaerts, J., Leung, L. R., Lipscomb, W. H., Lu, Y., Pandey, A., Pelletier, J. D., Perket, J., Randerson, J. T., Ricciuto, D. M., Sanderson, B. M., Slater, A., Subin, Z. M., Tang, J., Thomas, R. Q., Val Martin, M., and Zeng, X.: The Community Land Model Version 5: Description of New Features, Benchmarking, and Impact of Forcing Uncertainty, J. Adv. Model. Earth Sy., 11, 4245–4287, https://doi.org/10.1029/2018MS001583, 2019.

Li, H., Wigmosta, M. S., Wu, H., Huang, M., Ke, Y., Coleman, A. M., and Leung, L. R.: A Physically Based Runoff Routing Model for Land Surface and Earth System Models, J. Hydrometeorol., 14, 808–828, https://doi.org/10.1175/JHM-D-12-015.1, 2013.

Link, P. M., Scheffran, J., and Ide, T: Conflict and cooperation in the water-security nexus: a global comparative analysis of river basins under climate change, WIREs Water, 3, 495–515, https://doi.org/10.1002/wat2.1151, 2016.

Lipson, M. J., Grimmond, S., Best, M., Abramowitz, G., Coutts, A., Tapper, N., Baik, J. J., Beyers, M., Blunn, L., Boussetta, S., and Bou-Zeid, E.: Evaluation of 30 urban land surface models in the Urban-PLUMBER project: Phase 1 results, Q. J. Roy. Meteor. Soc., 150, 126–169, https://doi.org/10.1002/qj.4589, 2023.

Liu, J., Yang, H., Gosling, S. N., Kummu, M., Flörke, M., Pfister, S., Hanasaki, N., Wada, Y., Zhang, X., Zheng, C., Alcamo, J., and Oki, T.: Water scarcity assessments in the past, present, and future, Earth's Future, 5, 545–559, https://doi.org/10.1002/2016EF000518, 2017.

Liu, W., Sun, F., Lim, W. H., Zhang, J., Wang, H., Shiogama, H., and Zhang, Y.: Global drought and severe drought-affected populations in 1.5 and 2 °C warmer worlds, Earth Syst. Dynam., 9, 267–283, https://doi.org/10.5194/esd-9-267-2018, 2018.

Liu, Y., Hejazi, M., Kyle, P., Kim, S. H., Davies, E., Miralles, D. G., Teuling, A. J., He, Y., and Niyogi, D.: Global and Regional Evaluation of Energy for Water, Environ. Sci. Technol., 50, 9736–9745, https://doi.org/10.1021/acs.est.6b01065, 2016.

Lombardozzi, D. L., Lu, Y., Lawrence, P. J., Lawrence, D. M., Swenson, S., Oleson, K. W., Wieder, W. R., and Ainsworth, E. A.: Simulating Agriculture in the Community Land Model Version 5, J. Geophys. Res.-Biogeo., 125, e2019JG005529, https://doi.org/10.1029/2019JG005529, 2020.

Mancosu, N., Snyder, R., Kyriakakis, G., and Spano, D.: Water Scarcity and Future Challenges for Food Production, Water, 7, 975–992, https://doi.org/10.3390/w7030975, 2015.

Manju, S. and Sagar, N.: Renewable energy integrated desalination: A sustainable solution to overcome future fresh-water scarcity in India, Renewable and Sustainable Energy Reviews, 73, 594–609, https://doi.org/10.1016/j.rser.2017.01.164, 2017.

Mankin, J. S., Seager, R., Smerdon, J. E., Cook, B. I., and Williams, A. P.: Mid-latitude freshwater availability reduced by projected vegetation responses to climate change, Nat. Geosci. 12, 983–988, https://doi.org/10.1038/s41561-019-0480-x, 2019.

McDermid, S., Nocco, M., Lawston-Parker, P., Keune, J., Pokhrel, Y., Jain, M., Jägermeyr, J., Brocca, L., Massari, C., Jones, A. D., Vahmani, P., Thiery, W., Yao, Y., Bell, A., Chen, L., Dorigo, W., Hanasaki, N., Jasechko, S., Lo, M.-H., Mahmood, R., Mishra, V., Mueller, N. D., Niyogi, D., Rabin, S. S., Sloat, L., Wada, Y., Zappa, L., Chen, F., Cook, B. I., Kim, H., Lombardozzi, D., Polcher, J., Ryu, D., Santanello, J., Satoh, Y., Seneviratne, S., Singh, D., and Yokohata, T.: Irrigation in the Earth system, Nat. Rev. Earth Environ., 4, 435–453, https://doi.org/10.1038/s43017-023-00438-5, 2023.

Mekonnen, M. M. and Hoekstra, A. Y.: Four billion people facing severe water scarcity, Sci. Adv., 2, e1500323, https://doi.org/10.1126/sciadv.1500323, 2016.

Milly, P. C. D., Betancourt, J., Falkenmark, M., Hirsch, R. M., Kundzewicz, Z. W., Lettenmaier, D. P., and Stouffer, R. J.: Sta-

tionarity Is Dead: Whither Water Management?, Science, 319, 573–574, https://doi.org/10.1126/science.1151915, 2008.

Mizukami, N., Clark, M. P., Sampson, K., Nijssen, B., Mao, Y., McMillan, H., Viger, R. J., Markstrom, S. L., Hay, L. E., Woods, R., Arnold, J. R., and Brekke, L. D.: mizuRoute version 1: a river network routing tool for a continental domain water resources applications, Geosci. Model Dev., 9, 2223–2238, https://doi.org/10.5194/gmd-9-2223-2016, 2016.

Mizukami, N., Clark, M. P., Gharari, S., Kluzek, E., Pan, M., Lin, P., Beck, H. E., and Yamazaki, D.: A vector-based river routing model for Earth system models: Parallelization and global applications, J. Adv. Model. Earth Sy., 13, e2020MS002434, https://doi.org/10.1029/2020MS002434, 2021.

Mount, J. F. and Hanak, E.: Water use in California, Public Policy Institute of California, 2019.

Mukhamedova, N. and Wegerich, K.: The feminization of agriculture in post-Soviet Tajikistan, J. Rural Stud., 57, 128–139, https://doi.org/10.1016/j.jrurstud.2017.12.009, 2018.

Müller Schmied, H., Cáceres, D., Eisner, S., Flörke, M., Herbert, C., Niemann, C., Peiris, T. A., Popat, E., Portmann, F. T., Reinecke, R., Schumacher, M., Shadkam, S., Telteu, C.-E., Trautmann, T., and Döll, P.: The global water resources and use model WaterGAP v2.2d: model description and evaluation, Geosci. Model Dev., 14, 1037–1079, https://doi.org/10.5194/gmd-14-1037-2021, 2021.

Nazemi, A. and Wheater, H. S.: On inclusion of water resource management in Earth system models – Part 1: Problem definition and representation of water demand, Hydrol. Earth Syst. Sci., 19, 33–61, https://doi.org/10.5194/hess-19-33-2015, 2015.

Nie, W., Zaitchik, B. F., Rodell, M., Kumar, S. V., Anderson, M. C., and Hain, C.: Groundwater Withdrawals Under Drought: Reconciling GRACE and Land Surface Models in the United States High Plains Aquifer, Water Resour. Res., 54, 5282–5299, https://doi.org/10.1029/2017WR022178, 2018.

Oki, T. and Kanae, S.: Global Hydrological Cycles and World Water Resources, Science 313, 1068–1072, https://doi.org/10.1126/science.1128845, 2006.

Pan, Y., Birdsey, R. A., Fang, J., Houghton, R., Kauppi, P. E., Kurz, W. A., Phillips, O. L., Shvidenko, A., Lewis, S. L., Canadell, J. G., Ciais, P., Jackson, R. B., Pacala, S. W., McGuire, A. D., Piao, S., Rautiainen, A., Sitch, S., and Hayes, D.: A Large and Persistent Carbon Sink in the World's Forests, Science, 333, 988–993, https://doi.org/10.1126/science.1201609, 2011.

Pastor, A. V., Ludwig, F., Biemans, H., Hoff, H., and Kabat, P.: Accounting for environmental flow requirements in global water assessments, Hydrol. Earth Syst. Sci., 18, 5041–5059, https://doi.org/10.5194/hess-18-5041-2014, 2014.

Pokhrel, Y. N., Hanasaki, N., Wada, Y., and Kim, H.: Recent progresses in incorporating human land-water management into global land surface models toward their integration into Earth system models, WIREs Water 3, 548–574, https://doi.org/10.1002/wat2.1150, 2016.

Prein, A. F., Langhans, W., Fosser, G., Ferrone, A., Ban, N., Goergen, K., Keller, M., Tölle, M., Gutjahr, O., Feser, F., and Brisson, E.: A review on regional convection-permitting climate modeling: Demonstrations, prospects, and challenges, Rev. Geophys., 53, 323–361, https://doi.org/10.1002/2014RG000475, 2015.

Rathore, L. S., Kumar, M., Hanasaki, N., Mekonnen, M. M., and Raghav, P.: Water scarcity challenges across urban regions with expanding irrigation, Environ. Res. Lett., 19, 014065, https://doi.org/10.1088/1748-9326/ad178a, 2024.

Rodell, M., Famiglietti, J. S., Wiese, D. N., Reager, J. T., Beaudoing, H. K., Landerer, F. W., and Lo, M.-H.: Emerging trends in global freshwater availability, Nature 557, 651–659, https://doi.org/10.1038/s41586-018-0123-1, 2018.

Rust, J. M.: The impact of climate change on extensive and intensive livestock production systems, Animal Frontiers, 9, 20–25, https://doi.org/10.1093/af/vfy028, 2019.

Sacks, W. J., Cook, B. I., Buenning, N., Levis, S., and Helkowski, J. H.: Effects of global irrigation on the near-surface climate, Clim. Dynam., 33, 159–175, https://doi.org/10.1007/s00382-008-0445-z, 2009.

Seto, K. C., Güneralp, B., and Hutyra, L. R.: Global forecasts of urban expansion to 2030 and direct impacts on biodiversity and carbon pools, P. Natl. Acad. Sci. USA, 109, 16083–16088, https://doi.org/10.1073/pnas.1211658109, 2012.

Shiklomanov, I. A.: Appraisal and Assessment of World Water Resources, Water International, 25, 11–32, https://doi.org/10.1080/02508060008686794, 2000.

Steinfeld, H., Gerber, P., Wassenaar, T. D., Castel, V., Rosales M., and de Haan, C.: Livestock's long shadow: environmental issues and options, Food and Agriculture Organization of the United Nations, Rome, 2006.

Sutanudjaja, E. H., van Beek, R., Wanders, N., Wada, Y., Bosmans, J. H. C., Drost, N., van der Ent, R. J., de Graaf, I. E. M., Hoch, J. M., de Jong, K., Karssenberg, D., López López, P., Peßenteiner, S., Schmitz, O., Straatsma, M. W., Vannametee, E., Wisser, D., and Bierkens, M. F. P.: PCR-GLOBWB 2: a 5 arcmin global hydrological and water resources model, Geosci. Model Dev., 11, 2429–2453, https://doi.org/10.5194/gmd-11-2429-2018, 2018.

Taranu, I. S.: Bridging the gap: a new module for human water use in the Community Earth System Model version 2.2 (Scripts), Zenodo [code], https://doi.org/10.5281/zenodo.10518803, 2024a.

Taranu, I. S.: Bridging the gap: a new module for human water use in the Community Earth System Model version 2.2 (Model and Experiments), Zenodo [code], https://doi.org/10.5281/zenodo.10579224, 2024b.

Taranu, I. S.: Bridging the gap: a new module for human water use in the Community Earth System Model version 2.2 (Data), Zenodo [data set], https://doi.org/10.5281/zenodo.10518843, 2024c.

Thiery, W., Davin, E. L., Lawrence, D. M., Hirsch, A. L., Hauser, M., and Seneviratne, S. I.: Present-day irrigation mitigates heat extremes, J. Geophys. Res.-Atmos., 122, 1403–1422, https://doi.org/10.1002/2016JD025740, 2017.

Trenberth, K.: Changes in precipitation with climate change, Clim. Res., 47, 123–138, https://doi.org/10.3354/cr00953, 2011.

Trenberth, K. E., Dai, A., Van Der Schrier, G., Jones, P. D., Barichivich, J., Briffa, K. R., and Sheffield, J.: Global warming and changes in drought, Nat. Clim. Change, 4, 17–22, https://doi.org/10.1038/nclimate2067, 2014.

UNESCO: The United Nations World Water Development Report 2021: Valuing Water, United Nations, 2021.

Vanderkelen, I., van Lipzig, N. P. M., Sacks, W. J., Lawrence, D. M., Clark, M. P., Mizukami, N., Pokhrel, Y., and Thiery, W.: Simulating the impact of global reservoir expansion on the present-day climate, J. Geophys. Res.-Atmos., 126, e2020JD034485, https://doi.org/10.1029/2020JD034485, 2021.

Vanderkelen, I., Gharari, S., Mizukami, N., Clark, M. P., Lawrence, D. M., Swenson, S., Pokhrel, Y., Hanasaki, N., van Griensven, A., and Thiery, W.: Evaluating a reservoir parametrization in the vector-based global routing model mizuRoute (v2.0.1) for Earth system model coupling, Geosci. Model Dev., 15, 4163–4192, https://doi.org/10.5194/gmd-15-4163-2022, 2022.

Van Vliet, M. T. H., Jones, E. R., Flörke, M., Franssen, W. H. P., Hanasaki, N., Wada, Y., and Yearsley, J. R.: Global water scarcity including surface water quality and expansions of clean water technologies, Environ. Res. Lett., 16, 024020, https://doi.org/10.1088/1748-9326/abbfc3, 2021.

Veldkamp, T. I. E., Zhao, F., Ward, P. J., De Moel, H., Aerts, J. C., Schmied, H. M., Portmann, F. T., Masaki, Y., Pokhrel, Y., Liu, X., and Satoh, Y.: Human impact parameterizations in global hydrological models improve estimates of monthly discharges and hydrological extremes: a multi-model validation study, Environ. Res. Lett., 13, 055008, https://doi.org/10.1088/1748-9326/aab96f, 2018.

Voisin, N., Liu, L., Hejazi, M., Tesfa, T., Li, H., Huang, M., Liu, Y., and Leung, L. R.: One-way coupling of an integrated assessment model and a water resources model: evaluation and implications of future changes over the US Midwest, Hydrol. Earth Syst. Sci., 17, 4555–4575, https://doi.org/10.5194/hess-17-4555-2013, 2013.

Vörösmarty, C. J., Green, P., Salisbury, J., and Lammers, R. B.: Global water resources: vulnerability from climate change and population growth, Science, 289, 284–288, https://doi.org/10.1126/science.289.5477.284, 2000.

Vörösmarty, C. J., McIntyre, P. B., Gessner, M. O., Dudgeon, D., Prusevich, A., Green, P., Glidden, S., Bunn, S. E., Sullivan, C. A., Liermann, C. R., and Davies, P. M.: Global threats to human water security and river biodiversity, Nature, 467, 555–561, https://doi.org/10.1038/nature09440, 2010.

Wada, Y.: Modeling Groundwater Depletion at Regional and Global Scales: Present State and Future Prospects, Surv. Geophys., 37, 419–451, https://doi.org/10.1007/s10712-015-9347-x, 2016.

Wada, Y., Van Beek, L. P. H., Van Kempen, C. M., Reckman, J. W. T. M., Vasak, S., and Bierkens, M. F. P.: Global depletion of groundwater resources, Geophys. Res. Lett. 37, L20402, https://doi.org/10.1029/2010GL044571, 2010.

Wada, Y., van Beek, L. P. H., and Bierkens, M. F. P.: Modelling global water stress of the recent past: on the relative importance of trends in water demand and climate variability, Hydrol. Earth Syst. Sci., 15, 3785–3808, https://doi.org/10.5194/hess-15-3785-2011, 2011a.

Wada, Y., Van Beek, L. P. H., Viviroli, D., Dürr, H. H., Weingartner, R., and Bierkens, M. F. P.: Global monthly water stress: 2, Water demand and severity of water stress, Water Resour. Res., 47, 2010WR009792, https://doi.org/10.1029/2010WR009792, 2011b.

Wada, Y., Van Beek, L. P. H., and Bierkens, M. F. P.: Nonsustainable groundwater sustaining irrigation: A global assessment, Water Resour. Res., 48, 2011WR010562, https://doi.org/10.1029/2011WR010562, 2012.

Wada, Y., Van Beek, L. P. H., Wanders, N., and Bierkens, M. F. P.: Human water consumption intensifies hydrological drought worldwide, Environ. Res. Lett., 8, 034036, https://doi.org/10.1088/1748-9326/8/3/034036, 2013.

Wada, Y., Flörke, M., Hanasaki, N., Eisner, S., Fischer, G., Tramberend, S., Satoh, Y., van Vliet, M. T. H., Yillia, P., Ringler, C., Burek, P., and Wiberg, D.: Modeling global water use for the 21st century: the Water Futures and Solutions (WFaS) initiative and its approaches, Geosci. Model Dev., 9, 175–222, https://doi.org/10.5194/gmd-9-175-2016, 2016.

Weedon, G. P., Balsamo, G., Bellouin, N., Gomes, S., Best, M. J., and Viterbo, P.: The WFDEI meteorological forcing data set: WATCH Forcing Data methodology applied to ERA-Interim reanalysis data, Water Resour. Res., 50, 7505–7514, https://doi.org/10.1002/2014WR015638, 2014.

World Bank: Beyond Scarcity: Water Security in the Middle East and North Africa, MENA Development Report, Washington, DC, World Bank, http://hdl.handle.net/10986/27659 (last access: 16 October 2024), 2017.

World Resources Institute: World Resources, 2000–2001: People and Ecosystems, the Fraying Web of Life. Vol. 9, World Resources Institute, 2000.

Wu, W.-Y., Lo, M.-H., Wada, Y., Famiglietti, J. S., Reager, J. T., Yeh, P. J.-F., Ducharne, A., and Yang, Z.-L.: Divergent effects of climate change on future groundwater availability in key mid-latitude aquifers, Nat. Commun., 11, 3710, https://doi.org/10.1038/s41467-020-17581-y, 2020.

Xiao, M., Udall, B., and Lettenmaier, D. P.: On the Causes of Declining Colorado River Streamflows, Water Resour. Res., 54, 6739–6756, https://doi.org/10.1029/2018WR023153, 2018.

Yan, H., Sun, N., Eldardiry, H., Thurber, T. B., Reed, P. M., Malek, K., Gupta, R., Kennedy, D., Swenson, S. C., Hou, Z., Cheng, Y., and Rice, J. S.: Large Ensemble Diagnostic Evaluation of Hydrologic Parameter Uncertainty in the Community Land Model Version 5 (CLM5), J. Adv. Model. Earth Sy., 15, e2022MS003312, https://doi.org/10.1029/2022MS003312, 2023.

Yao, Y., Vanderkelen, I., Lombardozzi, D., Swenson, S., Lawrence, D., Jägermeyr, J., Grant, L., and Thiery, W.: Implementation and Evaluation of Irrigation Techniques in the Community Land Model, J. Adv. Model. Earth Sy., 14, e2022MS003074, https://doi.org/10.1029/2022MS003074, 2022.

Yassin, F., Razavi, S., Elshamy, M., Davison, B., Sapriza-Azuri, G., and Wheater, H.: Representation and improved parameterization of reservoir operation in hydrological and land-surface models, Hydrol. Earth Syst. Sci., 23, 3735–3764, https://doi.org/10.5194/hess-23-3735-2019, 2019.

Yokohata, T., Kinoshita, T., Sakurai, G., Pokhrel, Y., Ito, A., Okada, M., Satoh, Y., Kato, E., Nitta, T., Fujimori, S., Felfelani, F., Masaki, Y., Iizumi, T., Nishimori, M., Hanasaki, N., Takahashi, K., Yamagata, Y., and Emori, S.: MIROC-INTEG-LAND version 1: a global biogeochemical land surface model with human water management, crop growth, and land-use change, Geosci. Model Dev., 13, 4713–4747, https://doi.org/10.5194/gmd-13-4713-2020, 2020.